



**Politecnico
di Torino**

Politecnico di Torino

Department of Mechanical and Aerospace Engineering

MSc Thesis
in Automotive Engineering

HUMAN BODY MODEL AND PASSIVE SAFETY OF AUTONOMOUS VEHICLES

ANALYSIS OF BIOMECHANICAL RESULTS AND STUDY OF INJURIES

Tutors

Prof. Eng. Alessandro Scattina

Prof. Eng. Giovanni Belingardi

Candidate

Haozhou Zhao

JULY/2021

Abstract

This thesis work is aimed at studying the passive safety of the autonomous vehicle, investigating the performance of the new methodologies developed by Jsol Corporation for studying human body injury and injury risk. In this aim, a series of simulations that are set in a FE environment are reproduced, including the R-point impact and the rear wheel axis impact, in which the offset impact crash tests are being performed by using a middle-size sedan model, and a moving deformable barrier as the impactor. In particular, the finite element HBM (human body model) being used in this thesis is the total human model for safety (THUMS) developed by Toyota Motor Corporation, and the simulations are carried out by using Computational resources provided by `hpc@polito`, which is a project of Academic Computing within the Department of Control and Computer Engineering at the Politecnico di Torino (<http://www.hpc.polito.it>). Once the simulations are accomplished, the biomechanical data is obtained, in the next step, the results are analysed by using the THUMS injury risk visualisation tool from Jsol corporation, which consists of two programs, CLI (command-line interface and web application). CLI program is used for extracting some data from LS-DYNA simulation results (`d3plot`) and generating the CSV files that can be read by the web application. The web application is used for visualizing the injury risk of HBM

TABLE OF CONTENTS

INDEX OF FIGURE.....	1
INDEX OF TABLE	4
Preface	5
Introduction.....	5
Roadmap	7
Chapter 1: Finite Element Models	9
1.1 Introduction	9
1.2 AE-MDB model	10
1.3 Vehicle model.....	11
1.4 Human body model [8]	12
Chapter 2: injury criteria and risk theory.....	14
2.1 Introduction	14
2.2 Abbreviate injury scale [11]	15
2.3 Main injury criteria in deterministic method [12].....	16
2.3.1 Head Injury Criteria (HIC)	16
2.3.2 Neck injury criteria (Nij).....	16
2.3.3 Tibia index (TI)	16
2.3.4 Viscous criterion (VC)	17
2.3 Probabilistic injury risk evaluation method	18
2.4.1 Introduction.....	18
2.4.2 Injury risk curve development [12][14][16].....	19
Chapter 3: Simulation scenarios and pre/post-process	21
3.1 Introduction	21
3.2 Crush simulation scenarios	21
3.2.1 settings of the trolley	21
3.2.1 settings of the exterior and interior environment	22
3.2.1 Sensors on the THUMS model.....	26
3.3 Description of the simulation settings and data process	27
3.3.1 data extraction with CLI program.....	27
3.3.2 Data analysis with injury risk visualisation web application.....	30
Chapter 4: Results.....	33
4.1 Overview	33
4.2 Energy balance	39
4.2 Injury risk analysis in different impact scenarios	42
4.3.1 Injury risk analysis on the head	42
4.3.2 Injury risk analysis on the neck.....	45

4.3.3 Injury risk analysis on the Thorax	46
4.3.4 Injury risk analysis on the abdomen and pelvis.....	55
4.3.4 Injury risk analysis on the upper extremity	59
4.3.4 Injury risk analysis on the lower extremity.....	60
4.3.4 Injury risk analysis on the internal organs.....	62
Chapter 5: conclusion	70
References.....	73

INDEX OF FIGURE

Figure 1 motor-vehicle deaths, injuries, and number of crashes by type of crash,2019.....	6
Figure 2 Thesis roadmap.....	8
Figure 3 Jsol THUMS injury risk visualisation tool.....	8
Figure 4 AE-MDB Finite Element Model.....	10
Figure 5 AE-MDB barrier details.....	10
Figure 6 FE model of Toyota Camry.....	11
Figure 7 THUMS evolution.....	12
Figure 8 THUMS model AM50 V4.1(left) and detail (right).....	12
Figure 9 Injury risk curve related to HIC.....	19
Figure 10 CSDM based risk of brain injuries for various severities.....	20
Figure 11 MPS based risk of brain injuries for various severity.....	20
Figure 12 R-point impact in LS-PP.....	21
Figure 13 Rear-impact (wheel axis) in LS-PP.....	22
Figure 14 Planar finite.....	23
Figure 15 Detail of the deformed seat cushion(left) seat cushion without deformation(right).....	23
Figure 16 Top the isometric and the section view of final position(top), details of the hands and the feet positioned(bottom).....	24
Figure 17 three-point seatbelt components.....	25
Figure 18 THUMS positioned with the seatbelt model.....	25
Figure 19 Set of sensors.....	26
Figure 20 example of the element group file.....	27
Figure 21 body regions (right).....	28
Figure 22 Example of injury risk web application.....	30
Figure 23 example of correspondence between injury risk curve (upper)and MPS history curve long time (lower).....	31
Figure 24 isometric view of the R-point impact at t=0ms(left) and 20ms (right).....	33
Figure 25 isometric view of the R-point impact at t=40ms(left) and 60ms (right).....	33
Figure 26 isometric view of the R-point impact at t=80ms(left) and 90ms (right).....	34
Figure 27 front view of the R-point impact at t = 0ms (left) and t = 20ms (right).....	34
Figure 28 front view of the R-point impact at t = 40ms (left) and t = 60ms (right).....	34
Figure 29 front view of the R-point impact at t = 80ms (left) and t = 90ms (right).....	35
Figure 30 isometric view of the rear impact at t=0ms(left) and 20ms (right).....	35
Figure 31 isometric view of the rear impact at t=40ms(left) and 60ms (right).....	35
Figure 32 isometric view of the rear impact at t=80ms(left) and 90ms (right).....	36
Figure 33 front view of the rear impact at t = 0ms (left) and t = 20ms (right).....	36
Figure 34 front view of the rear impact at t = 40ms (left) and t = 60ms (right).....	36
Figure 35 front view of the rear impact at t = 80ms (left) and t = 90ms (right).....	36
Figure 36 injury risk overview on the R-point impact.....	37
Figure 37 injury risk overview on rear impact.....	37
Figure 38 energy balance R-point impact.....	39
Figure 39 energy balance rear impact.....	39
Figure 40 energy ratio for R-point impact.....	41
Figure 41 energy ratio for rear impact.....	41
Figure 42 MPS log history of the brain on R-point impact (red) and rear impact(blue).....	42
Figure 43 injury risk of the brain on R-point impact (red) and rear impact(blue).....	42

Figure 44 injury risk of the skull on R-point impact (red) and rear impact(blue)	43
Figure 45 MPS log history of the skull on R-point impact (red) and rear impact(blue).....	43
Figure 46 injury risk of the facial bone on R-point impact (red) and rear impact (blue)	44
Figure 47 MPS log history of the facial bone on R-point impact (red) and rear impact (blue)	44
.....	44
Figure 48 MPS log history of the cervical spine on R-point impact (red) and rear impact (blue).....	45
Figure 49 Injury risk of the cervical spine on R-point impact (red) and rear impact (blue)....	45
Figure 50 MPS log history of the left-side clavicle on R-point impact (red) and rear impact (blue).....	46
Figure 51 MPS log history of the right-side clavicle on R-point impact (red) and rear impact (blue).....	46
Figure 52 Injury risk of the left-side clavicle on R-point impact (red) and rear impact (blue)	47
Figure 53 Injury risk of the left-side clavicle on R-point impact (red) and rear impact (blue)	47
Figure 54 MPS log history of the right-side scapula on R-point impact (red) and rear impact (blue).....	48
Figure 55 Injury risk of the right-side scapula on R-point impact (red) and rear impact (blue)	48
.....	48
Figure 56 MPS log history of the left-side scapula on R-point impact (red) and rear impact (blue).....	48
Figure 57 Injury risk of the left-side scapula on R-point impact (red) and rear impact (blue)	49
Figure 58 Maximum Injury risk of the right-side ribs on R-point impact (red) and rear impact (blue).....	50
Figure 59 Maximum Injury risk of the left-side ribs on R-point impact (red) and rear impact (blue).....	51
Figure 60 MPS log history of each rib on the left side of the R-point impact(upper) and rear impact (lower).....	51
Figure 61 MPS log history of each rib on the right side of the R-point impact(upper) and rear impact (lower).....	52
Figure 62 MPS log history of the sternum on the R-point impact (red) and the rear impact (blue).....	52
Figure 63 injury risk of the sternum	53
Figure 64 Injury risk of the thoracic spine on the R-point impact (red) and the rear impact (blue).....	53
Figure 65 MPS log history of the thoracic spine on the R-point impact (red) and the rear impact (blue).....	54
Figure 66 MPS log history of the right side pelvis on the R-point impact (red) and the rear impact (blue).....	55
Figure 67 MPS log history of the left side pelvis on the R-point impact (red) and the rear impact (blue).....	55
Figure 68 Injury risk of the left side pelvis on the R-point impact (red) and the rear impact (blue).....	56
Figure 69 Injury risk of the right-side pelvis on the R-point impact (red) and the rear impact (blue).....	56
Figure 70 MPS log history of the sacrum on the R-point impact (red) and the rear impact (blue).....	56
Figure 71 Injury risk of the sacrum on the R-point impact (red) and the rear impact (blue) ..	57
Figure 72 MPS log history of the lumbar spine on the R-point impact (red) and the rear impact (blue).....	57

Figure 73 Injury risk of the lumbar spine on the R-point impact (red) and the rear impact (blue).....	57
Figure 74 Injury risk of the humerus on the R-point impact (red) and the rear impact (blue).....	59
Figure 75 MPS log history of the humerus on the R-point impact (red) and the rear impact (blue).....	59
Figure 76 MPS log history of the right-side lower leg on the R-point impact (red) and the rear impact (blue).....	60
Figure 77 Injury risk of the right-side lower leg on the R-point impact (red) and the rear impact (blue).....	61
Figure 78 Injury risk of the left-side lower leg on the R-point impact (red) and the rear impact (blue).....	61
Figure 79 CSDM value of the heart along time on the R-point impact (red) and the rear impact (blue).....	62
Figure 80 CSDM value of the right side lung along time on the R-point impact (red) and the rear impact (blue).....	63
Figure 81 CSDM value of the left side lung along time on the R-point impact (red) and the rear impact (blue).....	63
Figure 82 CSDM value of the liver along time on the R-point impact (red) and the rear impact (blue).....	64
Figure 83 Injury risk of the liver on the R-point impact (red) and the rear impact (blue).....	64
Figure 84 CSDM value of the liver along time on the R-point impact (red) and the rear impact (blue).....	65
Figure 85 Injury risk value of the spleen on the R-point impact (red) and the rear impact (blue).....	65
Figure 86 CSDM value of the stomach along time on the R-point impact (red) and the rear impact (blue).....	66
Figure 87 Injury risk value of the stomach on the R-point impact (red) and the rear impact (blue).....	66
Figure 88 CSDM value of the left-side(lower) and right-side(upper)kidney on the R-point impact (red) and the rear impact (blue).....	67
Figure 89 Injury risk of the left-side(lower) and right-side(upper)kidney on the R-point impact (red) and the rear impact (blue).....	68
Figure 90 CSDM value of the intestine along time on the R-point impact (red) and the rear impact (blue).....	68
Figure 91 Injury risk value of the intestine on the R-point impact (red) and the rear impact (blue).....	69

INDEX OF TABLE

Table 1 AIS severity injury scale.....	15
Table 2 ratios of computing risk curves for AIS1+, AIS2+, AIS3+, AIS5+ based on known risk curve for AIS4+	19
Table 3 CSDM based risk curve equation	20
Table 4 MPS based risk curve equation.....	20
Table 5 reserved group name in element group file (left)	28
Table 6 criteria and parameters adopted for different body parts.....	38
Table 7 overall injury risk of the ribs on different AIS level.....	49
Table 8 injury risk on each rib for both scenarios	50

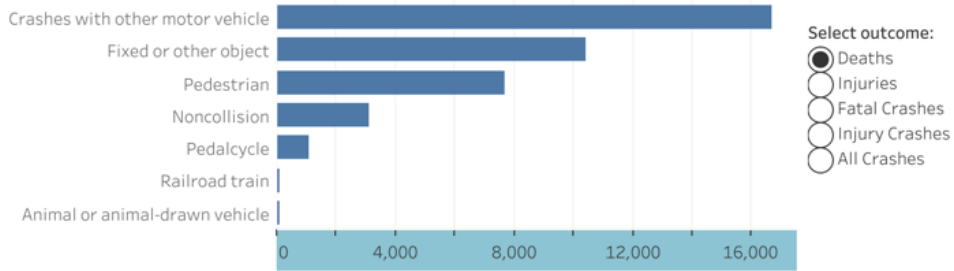
Preface

Introduction

Among all the types of motor-vehicle-related crashes, according to the study by an American non-profit safety advocate, National Safety Council, in 2019 collisions between two vehicles are the most happened scenario (43%), as shown in figure 1. Angle collisions are the most critical situation of death (about 7,500 in 2019), which is 44.9% [1]. Nearly 60% of the deaths are caused by thorax damage referring to the main causes of fatal injury [2]. Considering all these facts, it is necessary and urgent to study these causes scenarios, subsequently improving and developing more advanced passive/active security systems. Meanwhile, the study of the injury risk for the crash would help improve post-crash care, taking faster and more accurate actions after the crash. In that sense, the Euro NCAP program is developed, with a standard procedure to evaluate the performance against various safety threats for the new automobile designs to make the car safer [3]. However, NCAP is taking the measurement using the real vehicle, which is a high-expense experiment since the vehicle being tested will not be able to be reused. In this way the Finite Element Models would be a wise choice to be adopted for compromising this shortage, to better understand the mechanism of injury and the risk. In particular, the Human Body Model is a powerful instrument to illustrate the realistic response that the occupants experienced in the real crash test by providing higher quantity and more accurate data [4]. In this thesis, the finite element analysis methodology is adopted to study the injury risk of the occupants during the crash, in which two crash simulations, the R-point side impact and the rear wheel axis side impact, are performed by using Ls-Dyna. With the results of the simulations, a new tool developed by Jsol corporation is used for advanced analysis of the injury risk on each part of the human body.

Total Deaths: 39,107

Deaths by crash type



Crashes with other motor vehicles: Deaths



Figure 1 motor-vehicle deaths, injuries, and number of crashes by type of crash, 2019

Roadmap

As shown in figure 2, the roadmap diagram, to have an advanced injury risk analysis, the D3plot results from the Ls-Dyna simulation are required. The rear side and the middle side impact are simulated one by one on Ls-Dyna. Firstly, the whole simulation model was validated by using Ls-PrePost to make sure there is no errors. After this step, the specific keyword cards are added, and data is modified to acquire the data that is required for the further steps. Then the simulations are accomplished on the Ls-Dyna.

After the first simulation is accomplished, a necessary assessment of the simulation is done based on the energy balance for the simulation model, making sure this simulation is archived successfully. After this assessment, if the simulation is considered acceptable, the trolley is repositioned for the next scenario simulation. When both the simulation accomplished, Ls-Dyna result d3Plot of both scenarios is used to extract the desired data by using a command-line interface (CLI) application developed by Jsol corporation, and all the data required for the injury analysis is included in the CSV file being generated by CLI. Then CSV files are uploaded to the injury risk visualisation web application, for further analysis of the injury risk. In figure 3, the mechanism of the new develop injury analysis tool used in this thesis work is presented.

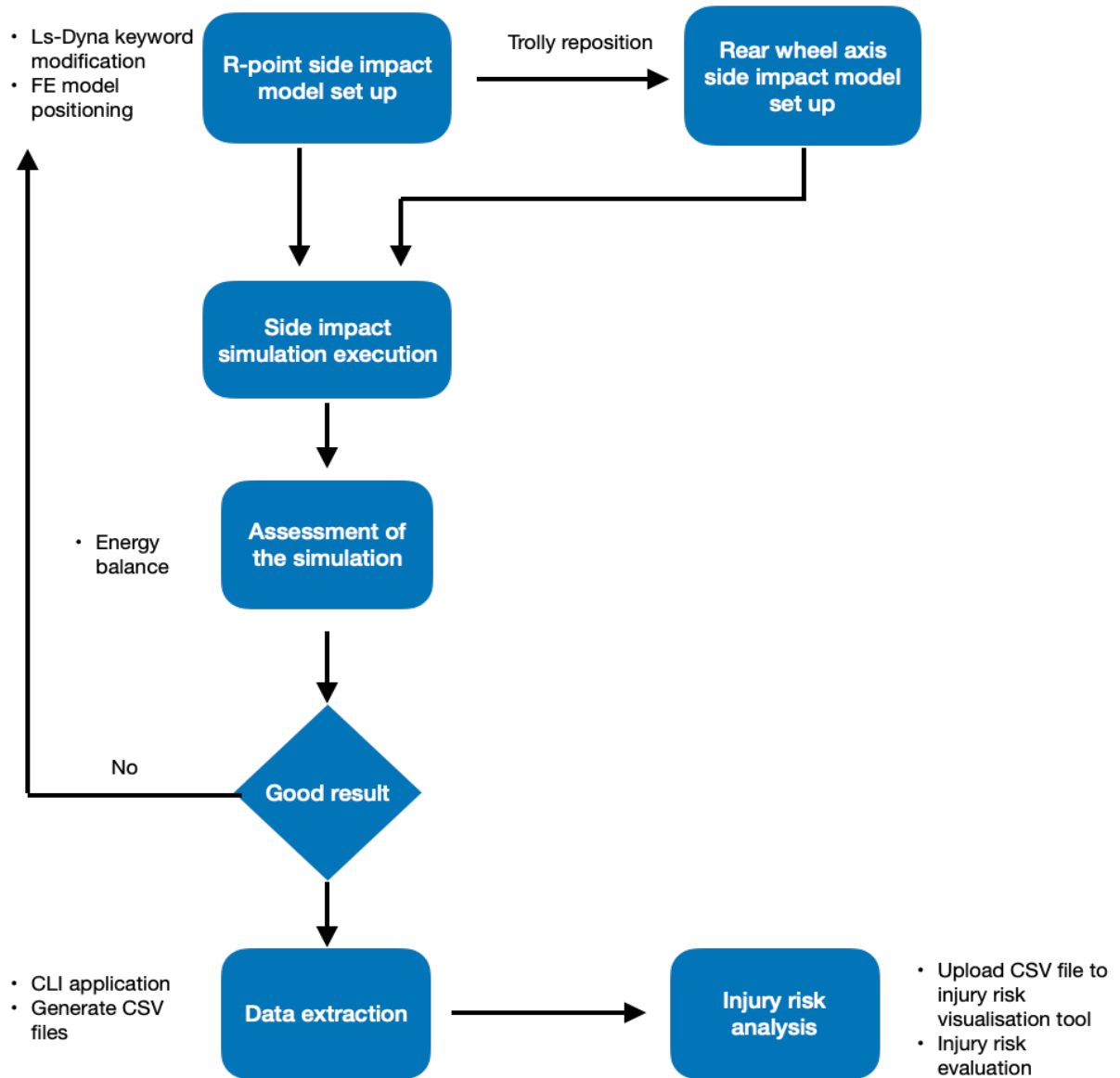


Figure 2 Thesis roadmap

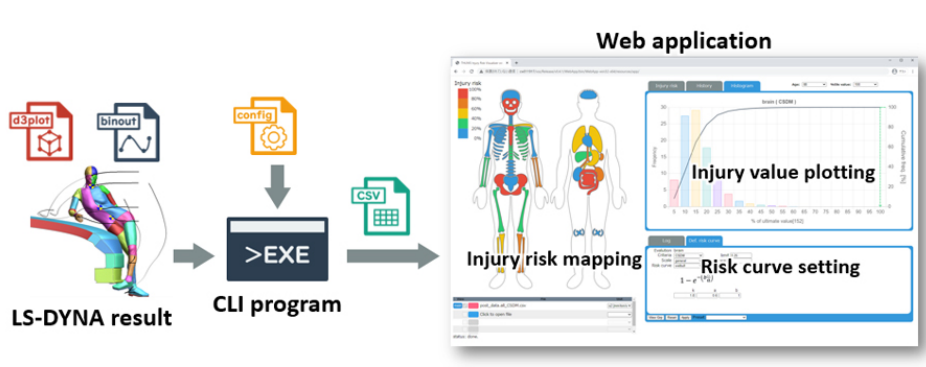


Figure 3 Jsol THUMS injury risk visualisation tool

Chapter 1: Finite Element Models

1.1 Introduction

In this thesis, three side impact simulations were done based on the Finite Element Models to predict the behaviours in real life during the crash. For predicting the fair accurate behaviour and acquiring desired data from the model, various tests must be performed to adjust the parameters of the model. Three main FEM are involved in the side-impact crash scenarios:

- A Human Body Model (HBM) is contained in the cabin and belted to simulate the behaviour of occupants. It is adopted to provide various outputs, including strains, acceleration, etc, to understand the severity and risk of injury
- A Vehicle Model, a 2012 Toyota Camry, which hosts the human body model during the crash
- A Mobile Deformable Barrier Model, as the impactor during the simulation, hits the vehicle in different positions with a velocity of 50 Km/h.

A short summarization of these three models is shown in the following sections.

1.2 AE-MDB model

In this thesis, the Advanced European Movable Barrier model used is developed by Livermore Software Technology Corporation (LSTC), which is based on the specification of AE-MDB version 1.0, produced by shell elements mainly, released on 26th February 2013, as shown in Figure 4.

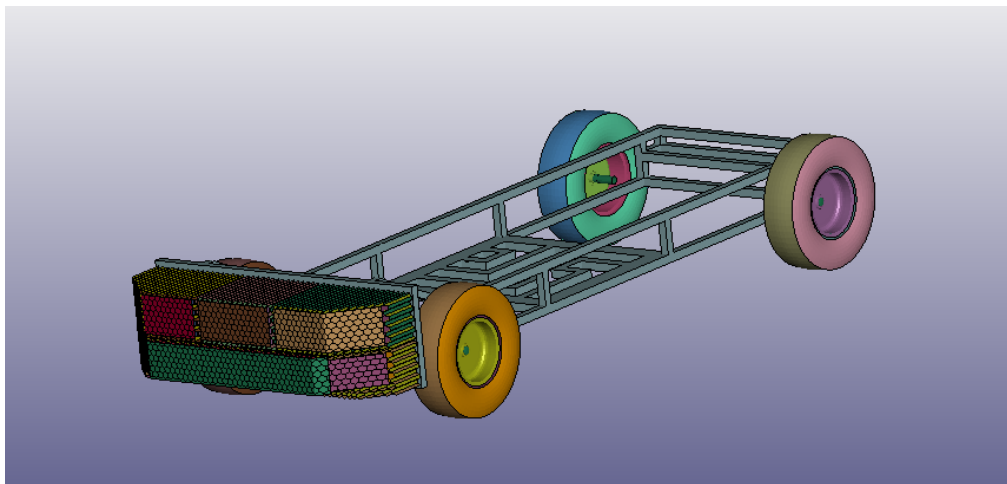


Figure 4 AE-MDB Finite Element Model

In this model, two parts are introduced: a trolley and an impactor. The impactor is composed of six single aluminium honeycomb blocks. During the simulation, they made it is reliable to increase the level of force progressively with the increasement of deflection. Additionally, a single element is attached of 60mm depth to the front of the lower row of blocks, and two aluminium plates are attached to the aluminium honey blocks from front and rear respectively [5]. As shown in Figure 5.

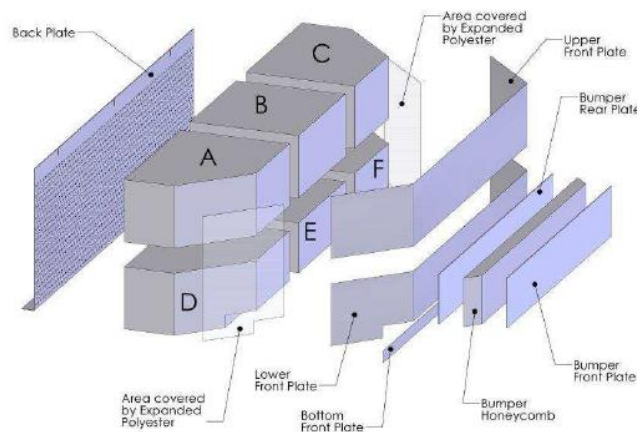


Figure 5 AE-MDB barrier details

1.3 Vehicle model

The vehicle model used for the crash simulation is a computer representation of a 2012 Toyota Camry mid-size passage sedan. Being developed by the Centre for Collision Safety and Analysis (CCSA) researchers by using a reverse engineering process under a contract with the federal highway administration. The vehicle finite element model is shown in Figure 6. The model contains 2.5 million elements, including specific details of the structure, derivation, and interior components which allows for the integration of occupant models for the simulation. [6]

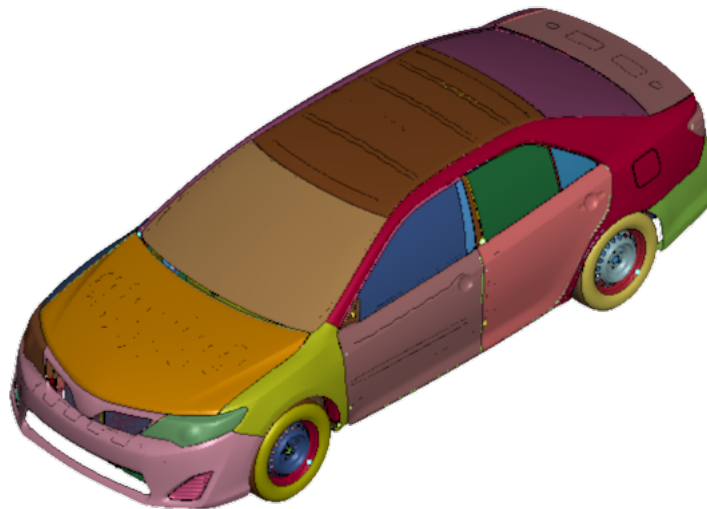


Figure 6 FE model of Toyota Camry

To fulfil the crash simulations in this thesis, further modification of the data in the finite element model is done. Originally the model was set to perform a frontal impact against a rigid wall at 35 mph (56.327kn/h). In this thesis, to confirm the regulation in Euro NCAP side-impact, the impacted vehicle must be firm, the velocity of the vehicle was deleted. Unite of the measure was modified from mm/ton/s to mm/kg/ms to be unified as the HBM and the Trolley [7].

1.4 Human body model [8]

THUMS, developed by Toyota Motor Corporation and Toyota Central R&D Labs, Inc., is the human body model used in this thesis. The acronym THUMS stands for the whole human model for safety. Several versions (Figure 7) were published and for the side-impact crash simulations in this thesis, the THUMS version being used is AM50 V4.1.

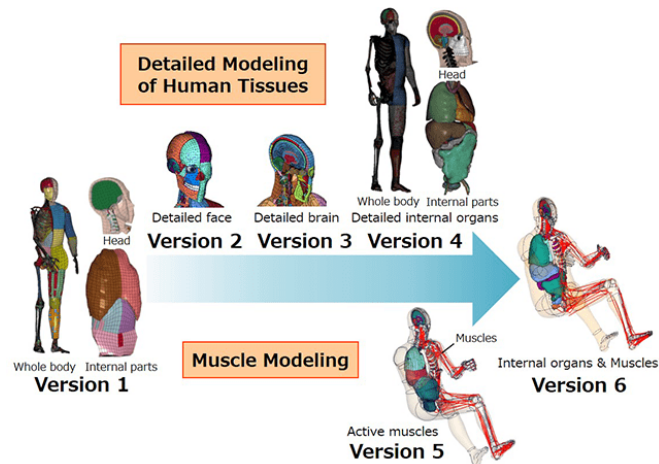


Figure 7 THUMS evolution

This THUMS model, AM50. V4.1 (Figure 8), is an average adult male model (AM50%ile), the height is 175cm, weight is 77kg, being developed aimed to simulate and study the kinematics and injury responses of the human body in the occupant crash simulation. The model has approximately 760,000 nodes and 1,9 million elements, it includes precise details

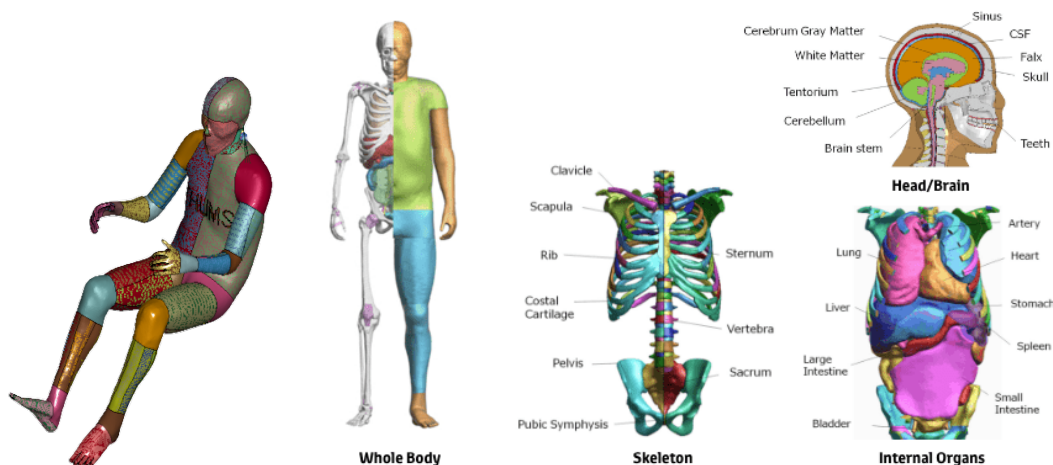


Figure 8 THUMS model AM50 V4.1(left) and detail (right)

about the head, the skeleton, internal organs, and air cavities. Therefore, it is possible for using this model to calculate the brain and internal organs injury at the tissue level, also the skeletal fracture and ligament injuries.

Chapter 2: injury criteria and risk theory

2.1 Introduction

The mechanical responses of crash test dummies were used to develop injury criteria. They are founded on an engineering theory that claims that the geometric and material features of a mechanical structure are the sole elements that regulate its interior reactions, regardless of size or material. Human surrogates were used to construct the criteria, which included both observable engineering traits and damage consequences [9]. In this thesis, a new method for evaluating the injury risk is adopted. Different from the main Injury Criteria (IC), which is going to be introduced in section 2.4, this new tool is using the strain-based probabilistic method to predict the injury risk and the injury risk curve will be plotted for the human body.

2.2 Abbreviate injury scale [11]

The Abbreviated Injury Scale (AIS), created by the Association for the Advancement of Automotive Medicine (AAAM), is the most widely used approach for characterising injuries. It defines the injuries of importance for the different scenarios. There are nine numbers to define the specific regions in the human body.

1. Head (Cranium and Brain)
2. Face, including eye and ear
3. Neck
4. Thorax
5. Abdomen and pelvic contents
6. Spine (Cervical, Thoracic, and Lumbar)
7. Upper extremity
8. Lower extremity, pelvis and buttocks
9. External (skin) and thermal injuries

Every injury in a specific region of the human body is assigned a score between 1 and 6 in the AIS, depending on its severity. As shown in Table 1.

ASI severity	injury
1	Minor
2	Moderate
3	Serious
4	Severe
5	Critical
6	Un-survivable

Table 1 AIS severity injury scale

For example, a fracture of the spine with cord involvement is a critical injury (AIS 5), a ruptured disc without nerve root damage is a moderate injury (AIS 2), and a severe injury (AIS 4) could be an incomplete cord syndrome.

2.3 Main injury criteria in deterministic method [12]

2.3.1 Head Injury Criteria (HIC)

For calculating the damage suffered by the head, one of the most widely used criteria is the Head Injury Criteria (HIC), it is computed in the formula:

$$HIC_{36} = (t_2 - t_1) \left(\left(\frac{1}{t_2 - t_1} \int_{t_1}^{t_2} a_r dt \right) \right)^{2.5} \quad (1)$$

Where:

- a_r resultant acceleration of the head
- 36 corresponding time interval length, 36 Ms.

2.3.2 Neck injury criteria (Nij)

For determining the injury criteria related to the neck, shearing forces at the transition from head to neck, the axial tensile force, and the axial compression force is used, and expressed in kN, with the duration measured in ms. The neck injury criteria value is calculated in the formula:

$$Nij = \frac{F_z}{F_{int}} + \frac{M_y}{M_{int}} \quad (2)$$

Where:

- F_z axial load from head to neck
- F_{int} critical value used for normalisation
- M_y bending moment
- M_{int} critical moment value used

2.3.3 Tibia index (TI)

For the lower leg area, the injury criteria being used is the Tibia index, for which the bending moments around the x and y-axis, and the axial pressure force in the z-direction at the top or bottom end of the tibia is considered.

The calculation equation of TI is:

$$TI = \left| \frac{M_R}{(M_c)_R} \right| + \left| \frac{F_Z}{(F_c)_Z} \right| \quad (3)$$

$$M_R = \sqrt{(M_x)^2 + (M_y)^2} \quad (4)$$

- M_x x-axis bending moment
- M_y y-axis bending moment
- $(M_c)_R$ critical bending moment
- $(F_c)_z$ z-direction critical compression force
- F_z z-direction axial compression force

2.3.4 Viscous criterion (VC)

The chest area, as one of the most suffered areas during the side-impact, Vicious criterion is adopted for assessing the injury risk for the soft tissue injury caused by crush mechanism. For the case of a side-impact, it will consider the rib deflections, which is calculated as:

$$VS = \textit{Scaling_factor} \frac{Y_{CFC180}}{Defconst} \frac{dY_{CFC180}}{dt} \quad (5)$$

In specific:

- *Scaling factor* function of the dummy type used in the simulation
- *Y* rib deflection
- $\frac{Y_{CFC180}}{Defconst}$ deformation velocity
- *Defconst* dummy constant

2.3 Probabilistic injury risk evaluation method

2.4.1 Introduction

In this thesis work, a newly developed tool is adopted for analysing the injury risk by Jsol Corporation. The method being used is a strain-based probabilistic fashion for predicting the injury risk of bones, brain and internal organs using the human whole-body finite element (FE) model, the injury risk curve is calculated according to the CSDM (cumulative strain damage measurement) and MPS (maximum principal strain), by using the survival analysis, where Weibull distribution (Equation 6) is used specifically. CSDM was developed as the first mechanical measure to evaluate the injury damage within the brain according to the strain data [15]. When the brain experiences the strain levels than the various specified levels, volume fractions are generated, CSDM monitors the accumulation of strain damage by calculating it, which is based on the maximum principal strain (MPS) [19]. MPS is estimated from a strain tensor obtained by integration of the rate of deformation.

$$injury\ risk = 1 - e^{-\left(\frac{x}{a}\right)^k} \quad (6)$$

Where k is the shape parameter and b and a is the scale for Weibull distribution.

For the development and scaling of the risk curve. All the ossature parts are estimated using MPS criteria parameters of the function are based on the study of Kemper 2005[12] and Forman 2012[14] for evaluating Bone-AIS 2+ and Bone-AIS 3+, for example, the skull, face, ribs, cervical spine, sacrum, etc. As for internal organs, CSDM is recommended, the parameters of the survival function are well defined, both CSDM and MPS criteria can be used for evaluating the injury risk curve of the brain by the study by Takhounts 2013 [16]. In the following sections, the study of the development of the risk curve for both criteria are delineated.

2.4.2 Injury risk curve development [12][14][16]

As mentioned in the 2.4.1 introduction section. The risk curves were constructed both for CSDM and MPS based on the Weibull distribution (Eq. 6).

For brain injury risk, according to the recently established AIS scale for anatomic brain injuries [10], this injury risk curve (Eq. 6) corresponds to an AIS 4+ brain injury. The risk curves for HIC (Figure 9) were utilised to derive additional levels of the abbreviated injury scale [17], assuming identical severity ratios between comparable risk curves for HIC and CSDM at 50 % risks.

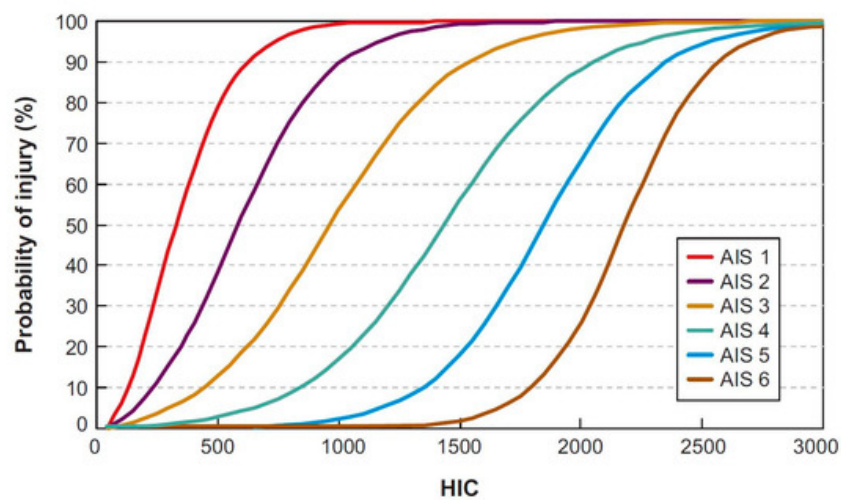


Figure 9 Injury risk curve related to HIC

To produce an AIS 3+ risk curve for CSDM, for example, the ratio (β_{34}), of AIS 3+/AIS 4+ risk curves at 50% for HIC was discovered, and then the AIS4+ risk curve for CSDM at 50% was multiplied by this ratio to obtain a 50% risk point for the AIS3+ CSDM:

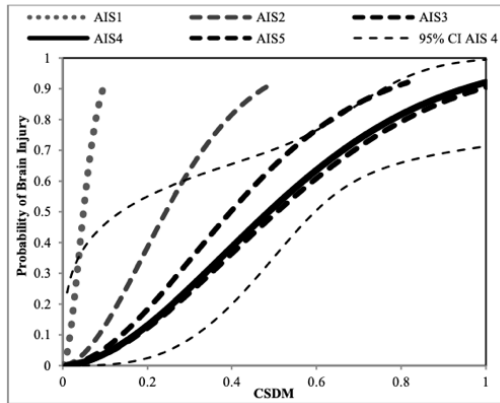
$$\text{CSMD AIS 3+ (50\%)} = \beta_{34} * \text{CSDM AIS 4+ (50\%)} \quad (7)$$

Combining equations 6 and 7, the CSDM risk curve for AIS3+ can be estimated, while the shape parameter k of the Weibull distribution is kept constant. In Table 2, the ratio β_{i4} is reproduced from Takhounts el al. 2011.

β_{14}	β_{24}	β_{34}	β_{54}
0.1	0.5	0.82	1.04

Table 2 ratios of computing risk curves for AIS1+, AIS2+, AIS3+, AIS5+ based on known risk curve for AIS4+

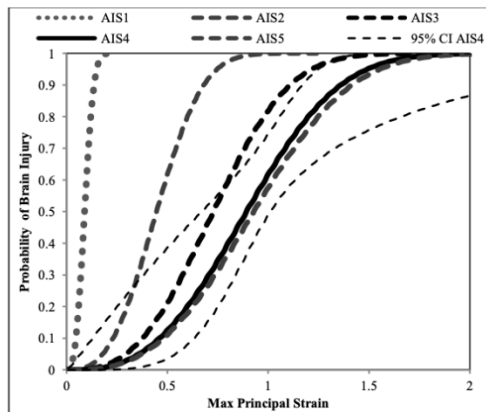
A set of risk curves and equations for CSDM can be obtained by scaling the AIS4+ risk curve at a level of 50% probability using the coefficients shown in Table 2, Figure 10, and Table 3. The risk curve based on MPS is obtained with a similar procedure (Figure 11 and Table 4)



$P(AIS\ 1) = 1 - e^{-\left(\frac{CSDM}{0.060}\right)^{1.8}}$
$P(AIS\ 2) = 1 - e^{-\left(\frac{CSDM}{0.300}\right)^{1.8}}$
$P(AIS\ 3) = 1 - e^{-\left(\frac{CSDM}{0.490}\right)^{1.8}}$
$P(AIS\ 4) = 1 - e^{-\left(\frac{CSDM}{0.600}\right)^{1.8}}$
$P(AIS\ 5) = 1 - e^{-\left(\frac{CSDM}{0.624}\right)^{1.8}}$

Figure 10 CSDM based risk of brain injuries for various severities.

Table 3 CSDM based risk curve equation



$P(AIS\ 1) = 1 - e^{-\left(\frac{MPS}{0.101}\right)^{2.84}}$
$P(AIS\ 2) = 1 - e^{-\left(\frac{MPS}{0.505}\right)^{2.84}}$
$P(AIS\ 3) = 1 - e^{-\left(\frac{MPS}{0.828}\right)^{2.84}}$
$P(AIS\ 4) = 1 - e^{-\left(\frac{MPS}{1.010}\right)^{2.84}}$
$P(AIS\ 5) = 1 - e^{-\left(\frac{MPS}{1.050}\right)^{2.84}}$

Figure 11 MPS based risk of brain injuries for various severity

Table 4 MPS based risk curve equation

As for the bones, the injury risk Weibull distribution parameters are estimated based on the bone fracture study by Kemper, 2005 [12]. In which the shape parameter k is 3.013, scale a is 0.0275. Internal organs have shape parameters K equals 1.8 and the scale A equal 0.6162, like the CSDM based brain injury AIS4+ risk curve.

Chapter 3: Simulation scenarios and pre/post-process

3.1 Introduction

To recreate the reality of the side crash with barrier, finite element simulation is used. In all the simulation scenarios in this thesis, the protocol of Euro NCAP is followed in the setting of the simulation environment: the velocity and position of the trolley, and the position of THUMS. After the simulation by using Ls-Dyna, the data desired will be extracted and analysed.

3.2 Crush simulation scenarios

3.2.1 settings of the trolley

Two different crush scenarios were simulated in this thesis as a respective comparison to study the injury conditions difference between the strike positions of the trolley to the vehicle. In the first one, the middle plane of the trolley is aligned to the R-point concerning the HBM, which strikes perpendicularly to the left side of the vehicle model, as shown in Figure 12.



Figure 12 R-point impact in LS-PP

In the second simulation, the trolley is positioned perpendicular to the car as in the first simulation but strikes to the rear wheel axis , as shown in Figure 13.

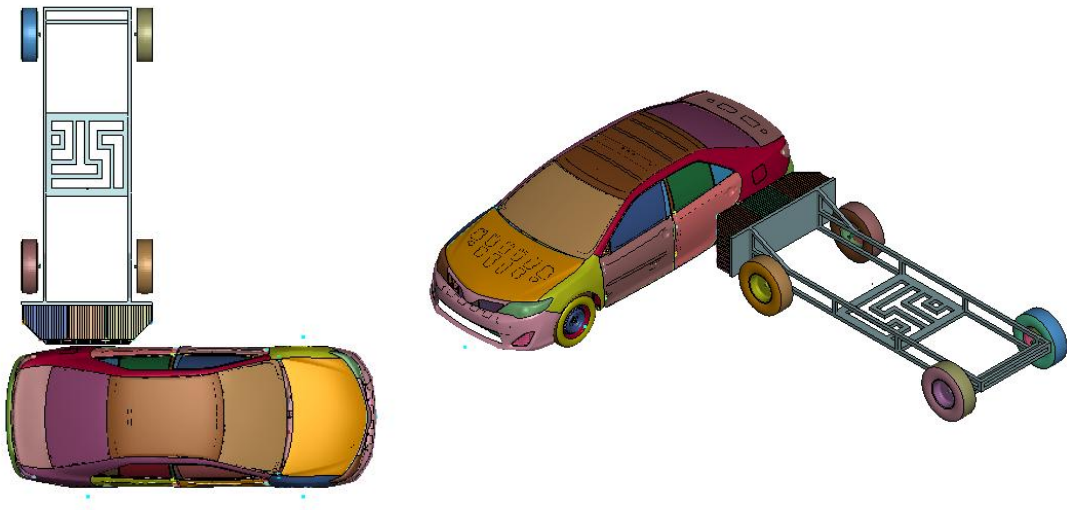


Figure 13 Rear-impact (wheel axis) in LS-PP

3.2.1 settings of the exterior and interior environment

According to the requirement of Euro NCAP, during the simulation the vehicle is stationary. The trolley with the moving deformable barrier impacts the vehicle from the side with a velocity of 50 km/h. It is set with the keyword `*INITIAL_VELOCITY` toward a `*NODE_SET` of the AE-MDB. The definition for the contact between the deformable barrier and the vehicle should be noticed. According to the recommendation from LS-Dyna, for the crash test, the keyword `*CONTACT_AUTOMATIC_SURFACE_TO_SURFACE` was used. The vehicle was set as slave, the barrier was set as master.

For the exterior environment, except for the trolley and vehicle, the ground is another important part that should be noticed. Keyword `*RIGIWALL_PLANER_FINITE` is added to create the ground to recreate the interactions between the wheels and the ground. The friction coefficient is set as 0.9 to represent the optimal situation of the tire grip. The group is shown in Figure 14

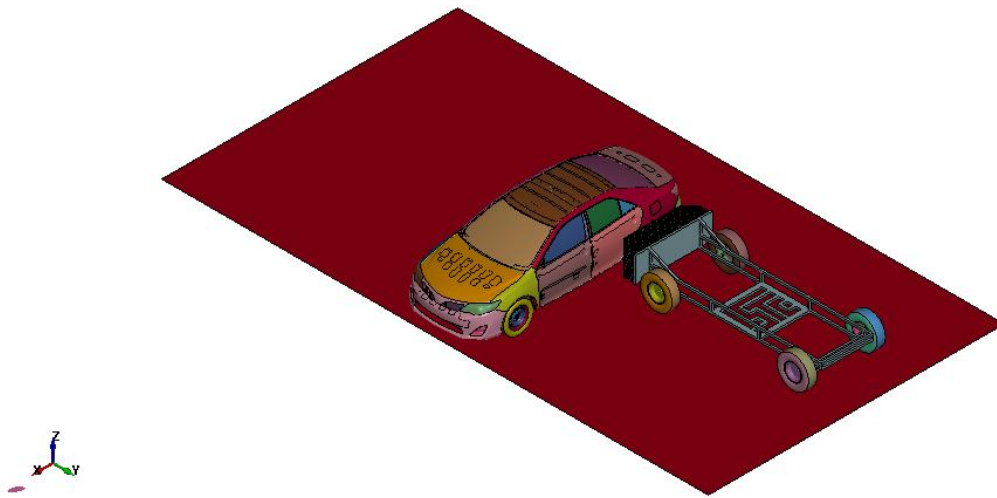


Figure 14 Planar finite

For the interior environment, three aspects were highlighted to guarantee an accurate simulation.

- The seat
- Position of the THUMS
- The seatbelt.

To represent reality, when an occupant is present inside the vehicle, the seat's cushion should be deformed due to the occupant's weight. Hence the seat deformation was considered when the human model was positioned upon it to avoid penetration during the simulation and better illustration of the real behaviour, as shown in figure 15.

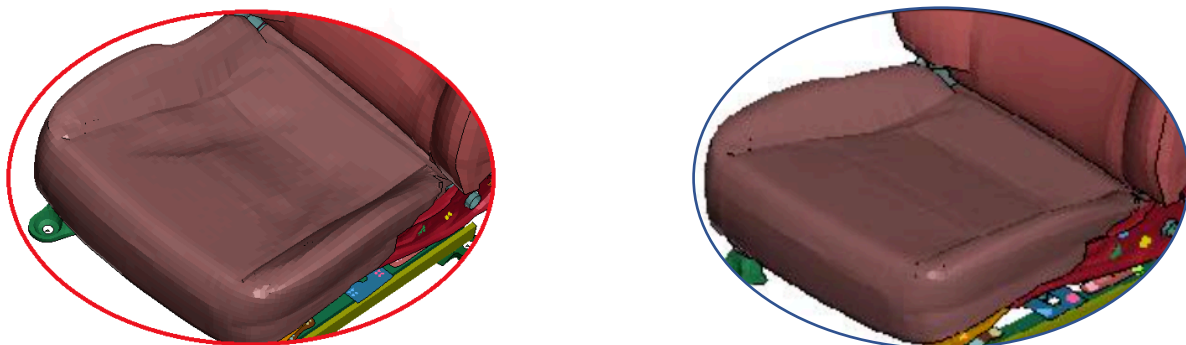


Figure 15 Detail of the deformed seat cushion(left) seat cushion without deformation(right)

The human model was positioned according to the legislation of Euro NCAP [3] as shown in figure 16. In particular, as described by Euro NCAP, the HBM was positioned by previous colleagues [7], the torso of the dummy was positioned as close as possible both to the driver seat and the H-point. The hands were set in contact with the steering wheel, on the position of the quarter to three. The left foot was in the rest position parallel to the floor since the footrest is not provided. The right foot was positioned on the acceleration pedal undepressed, the heel was in contact with the floor and set as far forward as possible, overlapping the pedal by at least 20mm.

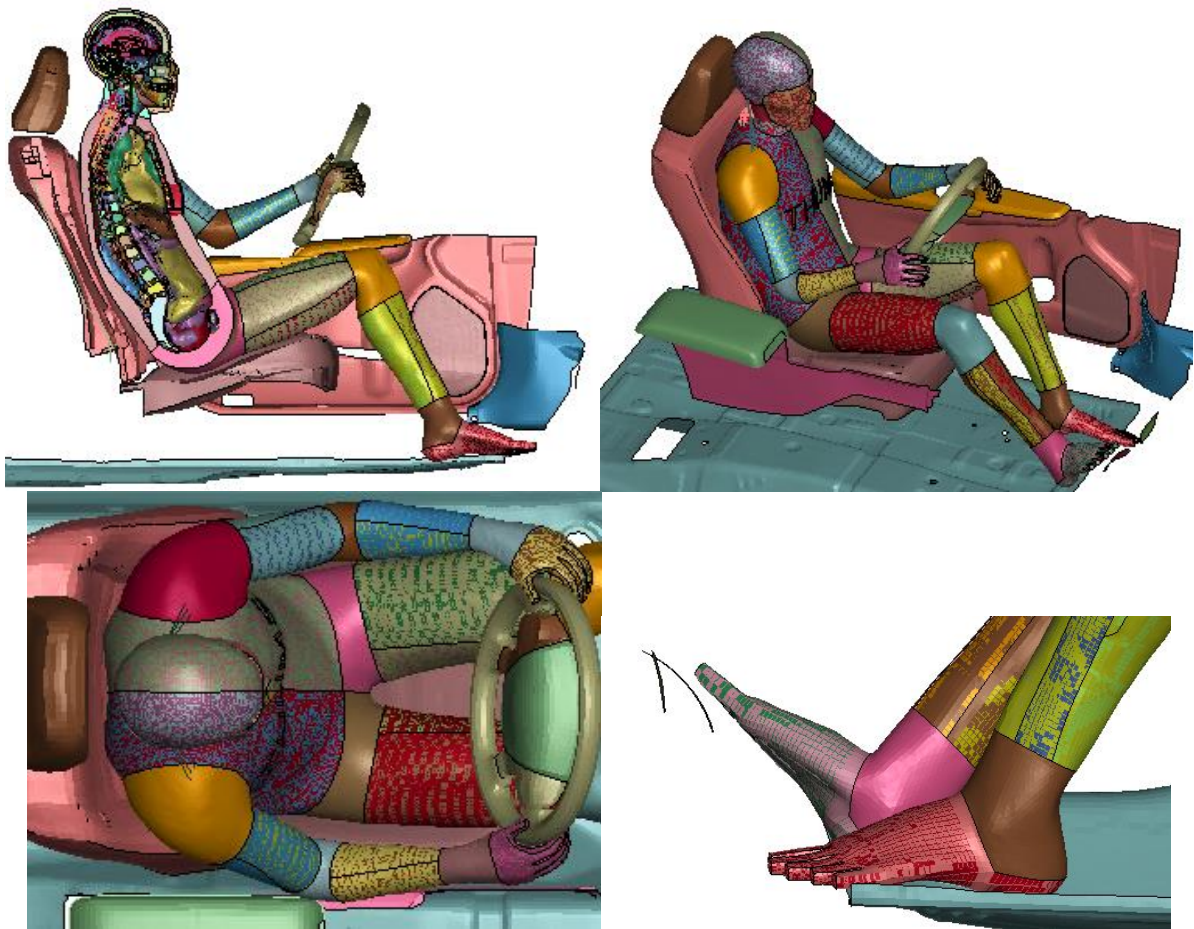


Figure 16 Top the isometric and the section view of final position(top), details of the hands and the feet positioned(bottom)

The last important aspect that should be considered is the seatbelt, the NCAP protocol states that the driver should be secured on the seatbelt during the crash test. In this thesis, the seatbelt used is a three-point seatbelt, composed of a B-pillar belt, a shoulder and torso belt, and a lap belt like the one in figure 17.

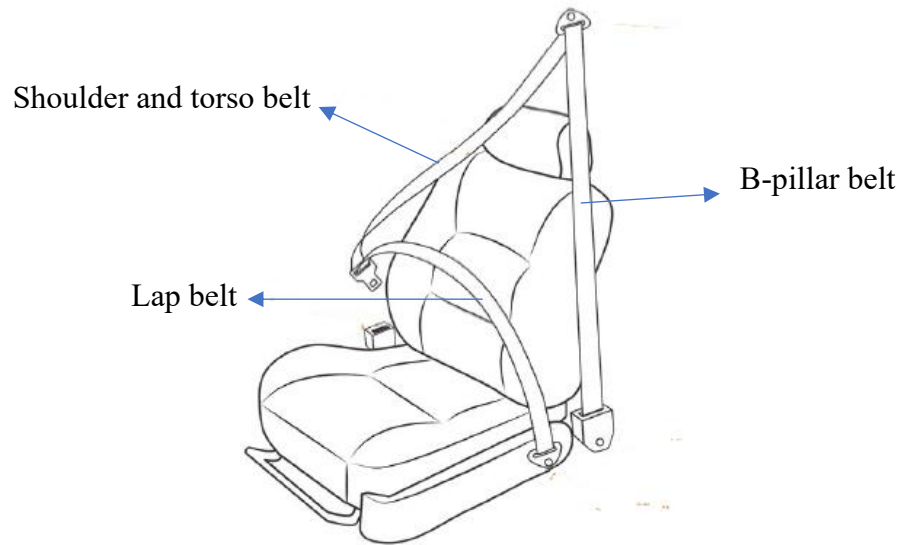


Figure 17 three-point seatbelt components

For recreating the reality in the vehicle, retractor, D-rings, sensor, and pretensioner were created and added with the seatbelt. The THUMS model with the seatbelt sitting in the vehicle can be seen in Figure 18.



Figure 18 THUMS positioned with the seatbelt model

Now the interior and exterior environments are all set and ready for the simulation.

3.2.1 Sensors on the THUMS model

The sensors are necessary to be included in the THUMS models to obtain the biomechanical results such as acceleration, velocity, displacements, forces, stress, strain, and energies, from the performed crash test simulations.

In this thesis work, the set of sensors on the THUMS model developed by Toyota Motors Corporation is not pre-installed. Sensors used in this work were made for previous activities by Germantti [18] and modified to better comply with the Euro NCAP requirements for the human model outputs [7]. The complete set of accelerometers and load sensors is shown in figure 19.

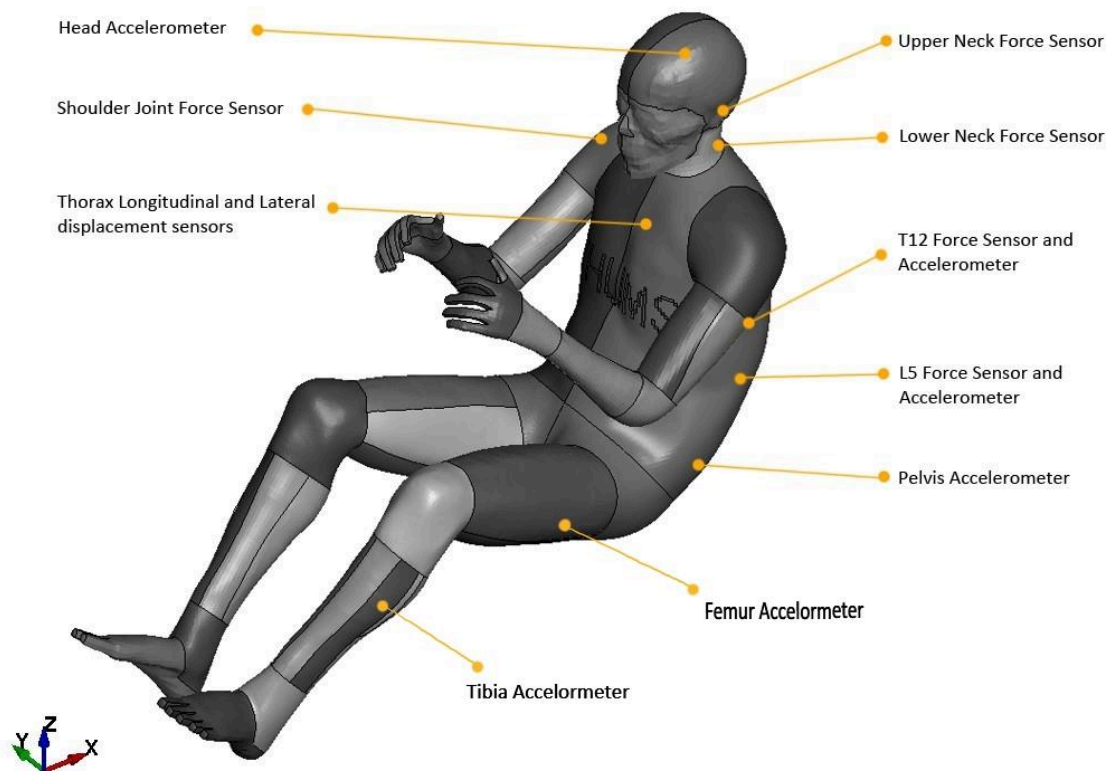


Figure 19 Set of sensors

3.3 Description of the simulation settings and data process

As mentioned before, the analysis of the injury risk for the human body is depending on the strain data. To get the strain data, keyword card *DATABASE_EXTENT_BINARY is added and modified. The *STRFLG should be turned on to write the directional strain tensors for solids, shells, and thick shells to the simulation result D3Plot. After the simulations were done, two applications were used for the post-processing of the simulation results for getting the injury risk analyses as introduced in Figure 3 in the roadmap section, which are:

- CLI (command-line interface) program
- Injury risk visualisation web application

3.3.1 data extraction with CLI program

The CLI application is aimed at extracting data from LS-DYNA results (d3plot) and creating the CSV file that contains the data that going to be used for the web application. Some files should be specified to use this program and get accurate information from d3plot.

1. Element group file
2. Group flag file

The element group file contains part id, element type, element id and element volume for each group, and is arranged in different blocks, an example of the groups of the body region is shown in figure 19 below, it can be observed that each region of the body is considered as a group, which contains varies parts made by the same or different elements.

```
$
#file
skull
$ ----- partID, type, elementID,volume
#data
88000002,SHELL,88200789, 5.058730244636536
88000002,SHELL,88200790, 5.817619442939758
$ ----- new file
#file
face
#data
88000022,SHELL,88215981, 56.64210319519043
88000022,SHELL,88215982, 48.16945838928223
$ ----- new file
#file
brain
#data
88000100,SOLID,88000000, 14.45948737637488
88000100,SOLID,88000001, 13.773450182713702
88000100,SOLID,88000002, 14.864120592044287
```

Figure 20 example of the element group file

The reserved group name and body regions are shown in Table 5 and Figure 20.

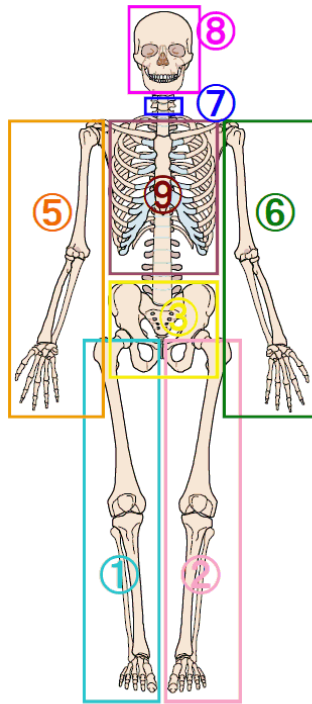


Figure 21 body regions (right)

No.	Body Region	Reserved group name
1	Lower Extremity - Right	femur_r, lower_leg_r, knee_ligament_r,
2	Lower Extremity - Left	femur_l, lower_leg_l, knee_ligament_l
3	Abdomen and Pelvis	pelvis_r, pelvis_l, sacrum, lumber_spine
4	Internal Organs	lung_r, lung_l, heart, aorta, liver, spleen, intestine, kidney_r, kidney_l, stomach
5	Upper Extremity - Right	humerus_r, forearm_r,
6	Upper Extremity - Left	humerus_l, forearm_l,
7	Neck	curvica_spine
8	Head	skull, face, brain
9	Thorax	clavicle_r, clavicle_l, scapula_r, scapula_l, rib_r01, rib_r02, rib_r03, rib_r04, rib_r05, rib_r06, rib_r07, rib_r08, rib_r09, rib_r10, rib_r11, rib_r12, rib_l01, rib_l02, rib_l03, rib_l04, rib_l05, rib_l06, rib_l07, rib_l08, rib_l09, rib_l10, rib_l11, rib_l12, sternum, thoracic_spine

Table 5 reserved group name in element group file (left)

It is important to match the element group file data with the version of the THUMS being used in the simulation otherwise the error will be announced. There are some default group element files being provided, in these simulations performed in this thesis, the file being used is [elem_group.AM50.v402.occ.txt], which is referring to the THUMS version 4.0.2 AM 50 occupants and higher version. If the THUMS model being used is not matching any of the files provided, the JavaScript provided along with the CLI application should be used with the ARUP primer for creating a matching file.

Some critical points should be noticed in this file to ensure accuracy before starting the data extraction process. The additional data blocks #entire_option to extract specific data of d3plot should be edited to ensure the quality of the data being extracted. In the default setting, the strain rate is written in the output CSV file by the CLI application as raw data, changing the calculation option (default = 0, filtered = 10) the strain rate and mises stress will be filtered with CFC180 Then the element group file is ready to be used.

The group flag file is another important aspect, it contains the group name and the flag value for indicating which group is desired to be processed, by default most of the flag value of the body group is 0, which means there will be no data extracted from this group, the flag value must be set to 1 for the groups are expected to be analysed.. A simple example of this file is shown below.

```
$
Skull,0
Face,0
Brain,1
```

This example indicates that only the data related to the brain is obtained during the data extraction process. In this thesis, the whole body is analysed, hence all the flags related to body groups will be set to 1. Then all the files required by the CLI program are prepared and ready for the data extraction process.

3.3.2 Data analysis with injury risk visualisation web application

As shown in Figure 3 in Roadmap, after using the CLI program, a CSV file will be generated, which contains the biomechanical data from the simulation as introduced in the previous section, the next step is using the injury risk visualisation web application for the further analysis. This Web application can visualize the injury risk on the HBM skeleton, show some criteria for risk evaluation and investigate a risk curve parameter. An example can be seen on Figure 22.

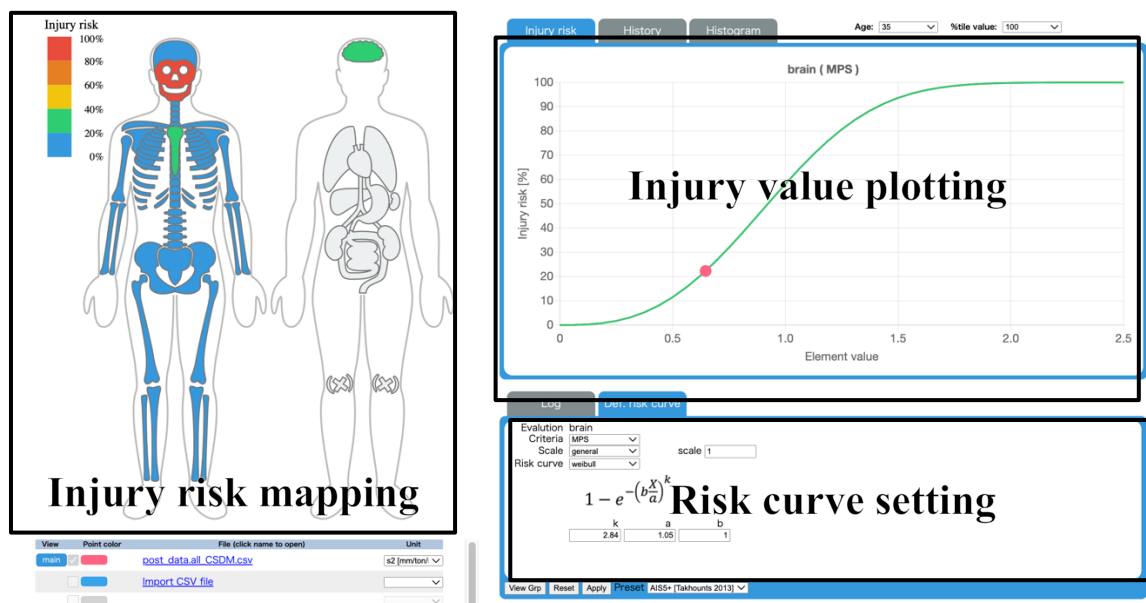


Figure 22 Example of injury risk web application

After uploading the CSV files that are generated by the CLI application to the application, the right units must be chosen, in this thesis work, the units complied with mm/kg/ms. In this web application, three main function areas can be observed.

1. Injury risk mapping

In this area, a compendious and straightforward view of the injury risk on each body part is presented, with a different colour corresponding to each injury risk interval. Among these injury risk intervals, five levels are distinguished, each of them with a 20% step, from 0 to 100%.

2. Injury value plotting

The injury value plotting area contains three main plotting windows, which are injury risk, history, and histogram. In the injury risk window, the risk curve is shown, the x-axis (element value) represents the maximum value of MPS or CSDM being calculated by the program along the time, and the y-axis represents the value of the injury risk value, which can be observed in figure 23.

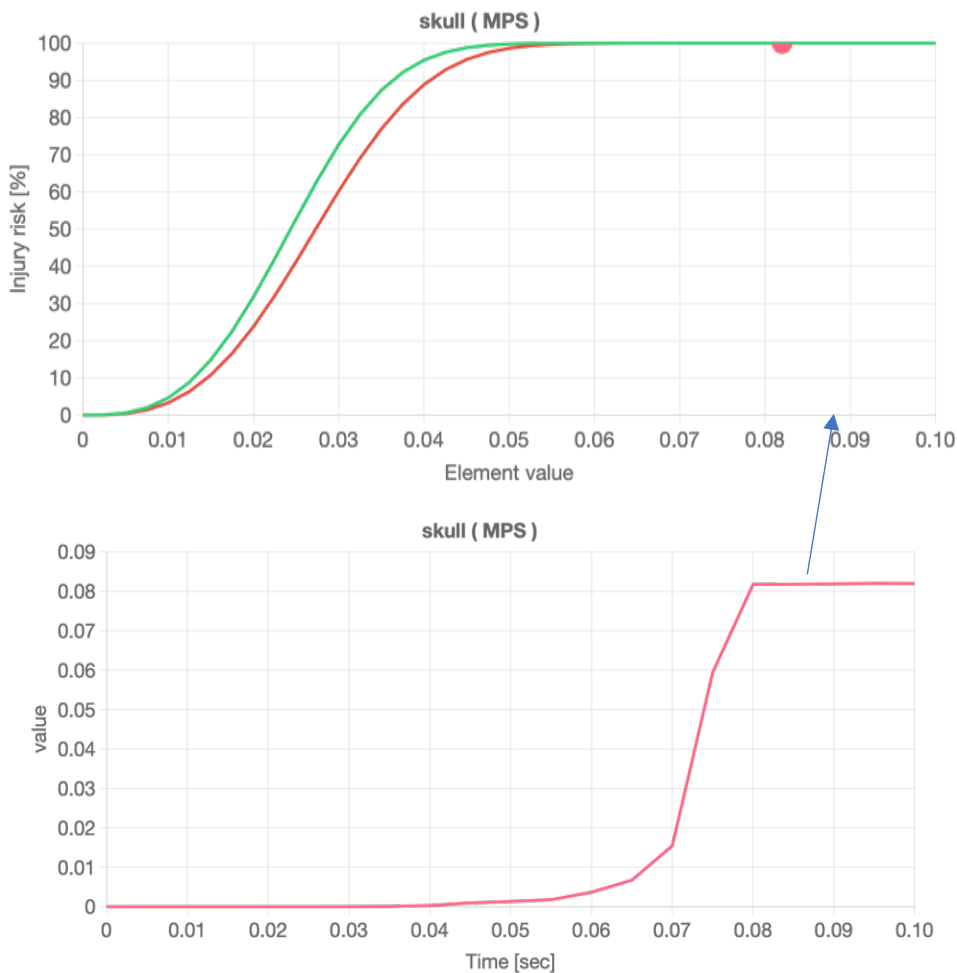


Figure 23 example of correspondence between injury risk curve (upper) and MPS history curve long time (lower)

As for the curve of risk, when the age scale is chosen, two different colour curves can be observed. The green one is representing the general scale despite the influence of age, and the red curve is the age-related risk curve, with the age changing, the injury risk varies at the same time.

3. Risk curve setting

In this window box, the theories of the corresponding body part to be applied to evaluate the risk curve are available to be selected. The log data can be viewed in this section.

In this web application, the CSDM of maximum principal strain for each human body part will be calculated automatically according to the input data from the CSV file. With the theory introduced in section 2.4, the risk curve is generated automatically. The corresponding injury risk is shown, in figure 23.

Chapter 4: Results

4.1 Overview

Once the models are prepared, the simulations are launched through the HPC physical cluster of Politecnico di Torino, it is a powerful instrument provided by Politecnico and corresponds to calculation resources and technical support for academic and didactic research activities employing centre systems. For both simulations, the cluster being used was the Legion cluster. After the simulation is accomplished, the results will be used for further analysis in the injury risk visualisation tool.

As for the R-point impact, Figures 24-26 below show the isometric views refereeing to time in ms. Figures 27-29 present the front section view of the R-point impact, to have a direct observation of the behaviour of the HBM.

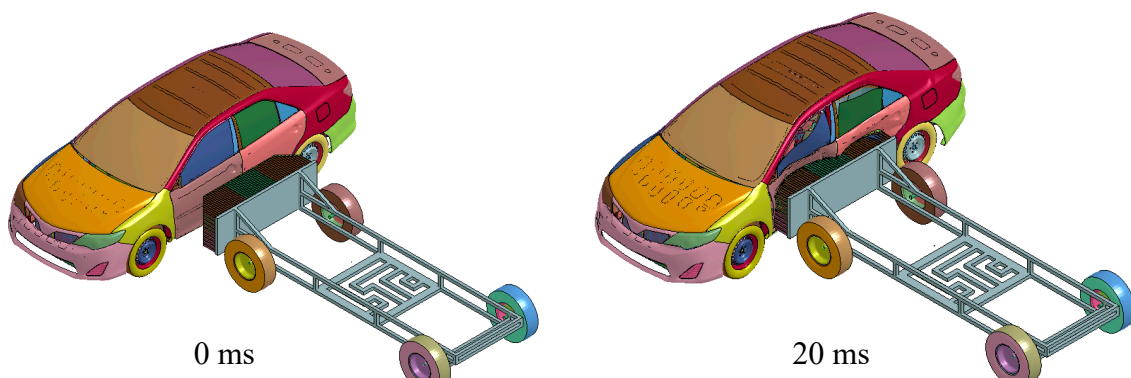


Figure 24 isometric view of the R-point impact at $t=0\text{ms}$ (left) and 20ms (right)

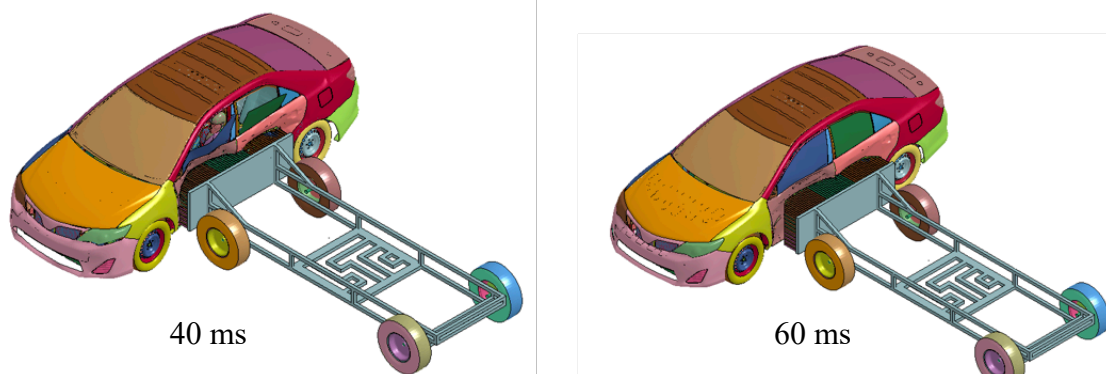
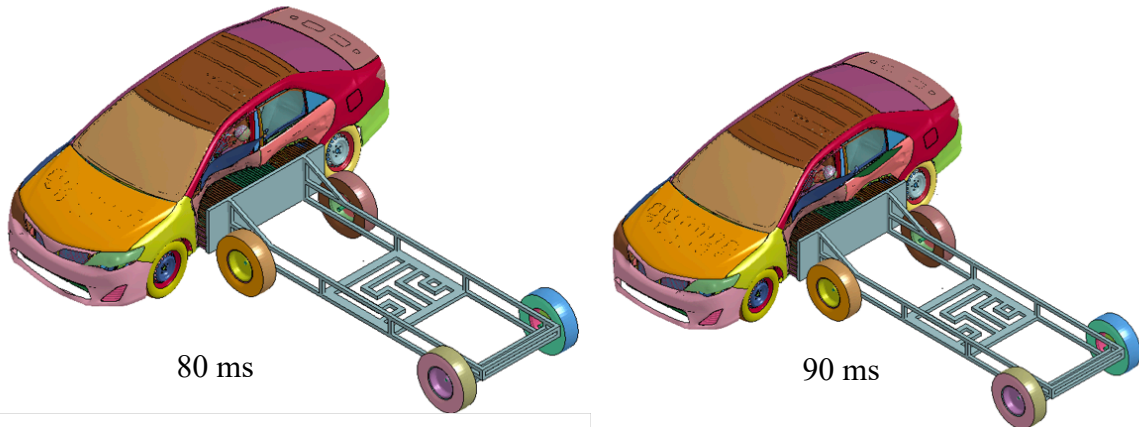


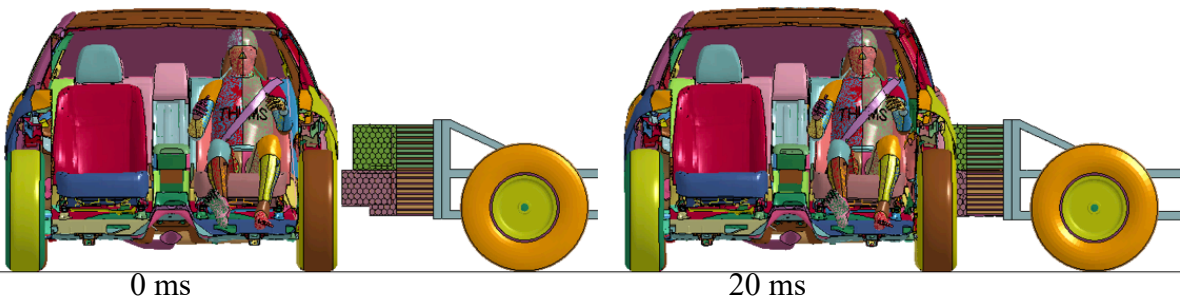
Figure 25 isometric view of the R-point impact at $t=40\text{ms}$ (left) and 60ms (right)



80 ms

90 ms

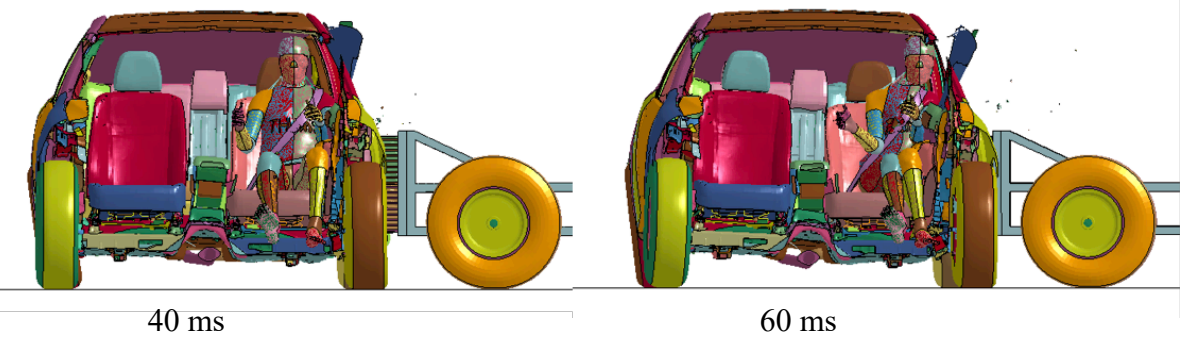
Figure 26 isometric view of the R-point impact at $t=80\text{ms}$ (left) and 90ms (right)



0 ms

20 ms

Figure 27 front view of the R-point impact at $t = 0\text{ms}$ (left) and $t = 20\text{ms}$ (right)



40 ms

60 ms

Figure 28 front view of the R-point impact at $t = 40\text{ms}$ (left) and $t = 60\text{ms}$ (right)

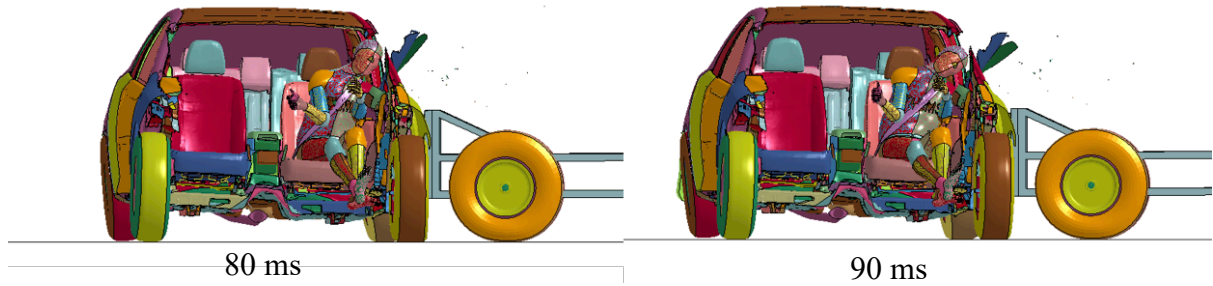


Figure 29 front view of the R-point impact at $t = 80\text{ms}$ (left) and $t = 90\text{ms}$ (right)

The rear impact as a comparison is present in the following figures. Same as the R-point impact the isometric view and a straightforward view of the behaviour of the THUMS will be presented.

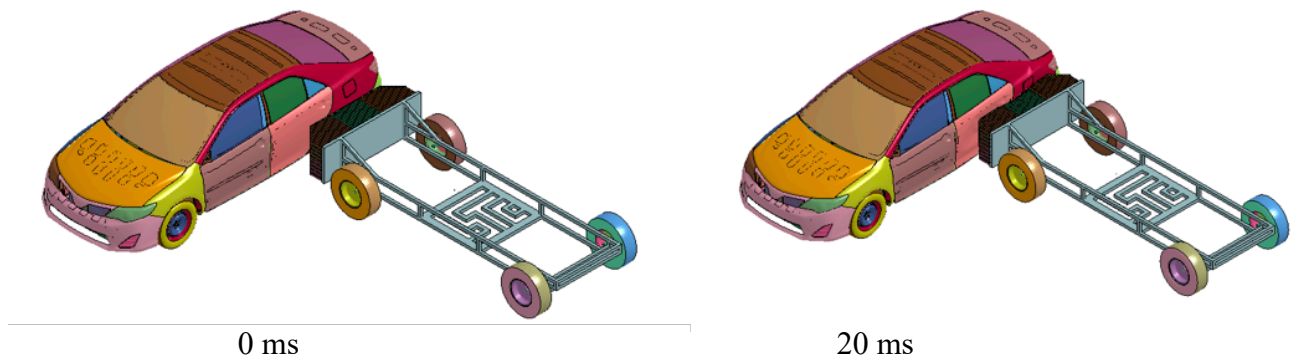


Figure 30 isometric view of the rear impact at $t=0\text{ms}$ (left) and 20ms (right)

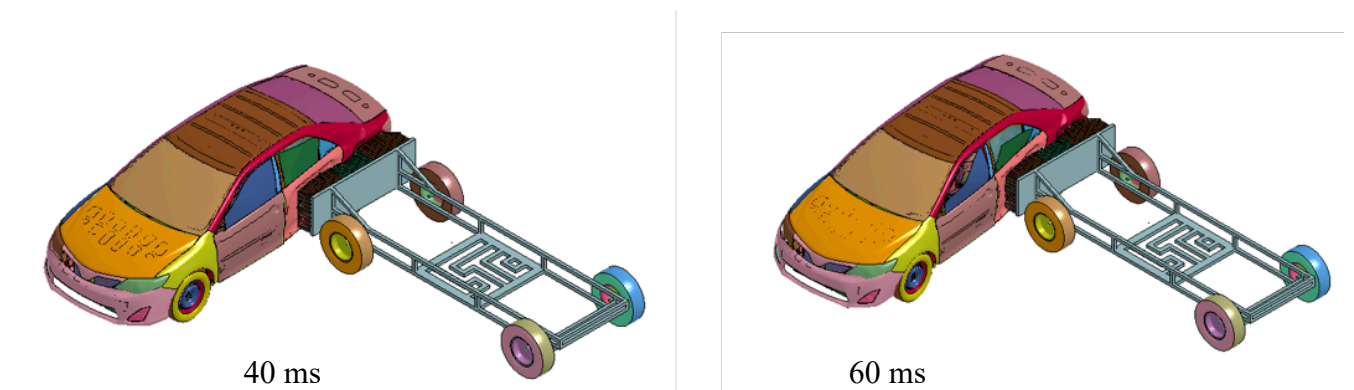


Figure 31 isometric view of the rear impact at $t=40\text{ms}$ (left) and 60ms (right)

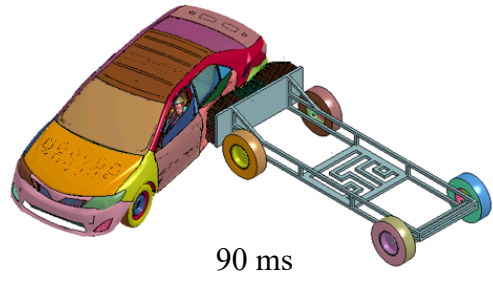
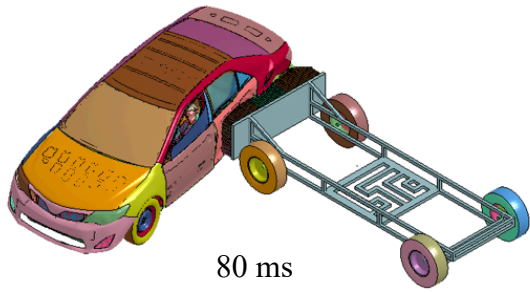


Figure 32 isometric view of the rear impact at $t=80\text{ms}$ (left) and 90ms (right)

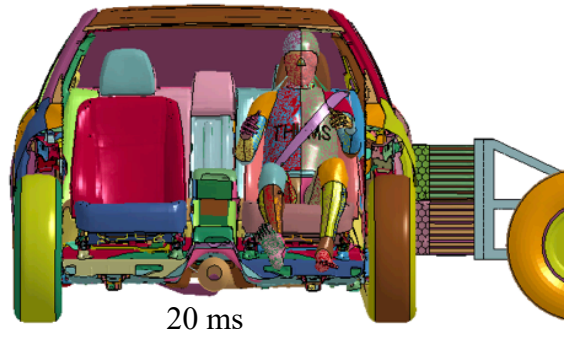
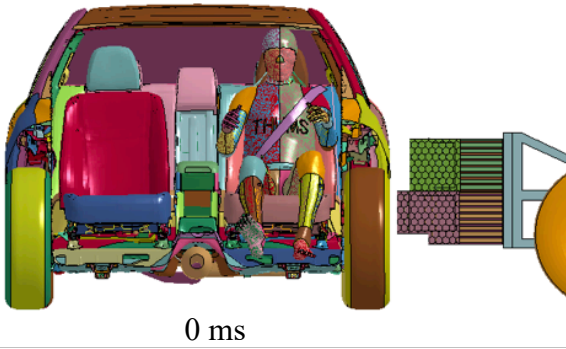


Figure 33 front view of the rear impact at $t = 0\text{ms}$ (left) and $t = 20\text{ms}$ (right)

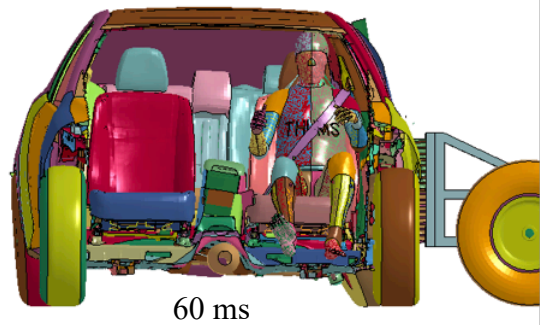
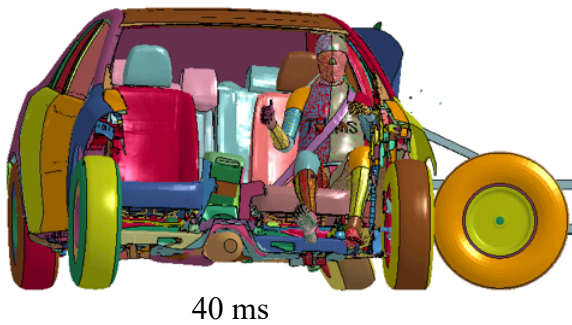


Figure 34 front view of the rear impact at $t = 40\text{ms}$ (left) and $t = 60\text{ms}$ (right)

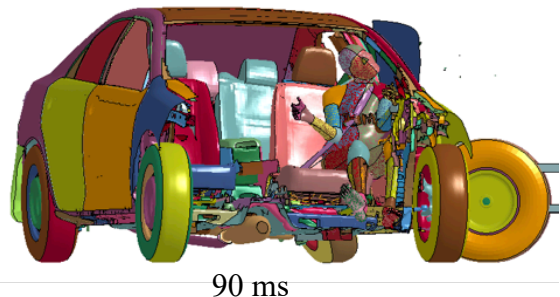
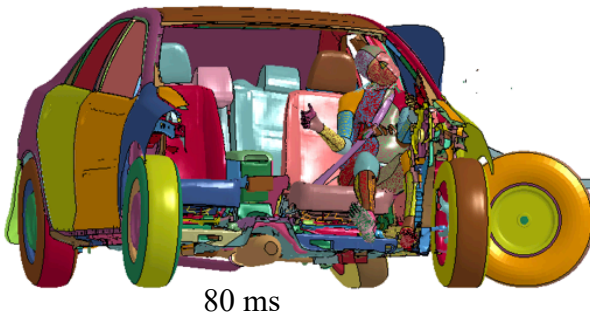


Figure 35 front view of the rear impact at $t = 80\text{ms}$ (left) and $t = 90\text{ms}$ (right)

In Figures 36 and 37, an overview of the injury risk visualisation tool is presented on the R-point and rear impact, which shows the injury risk on the skeleton scale.

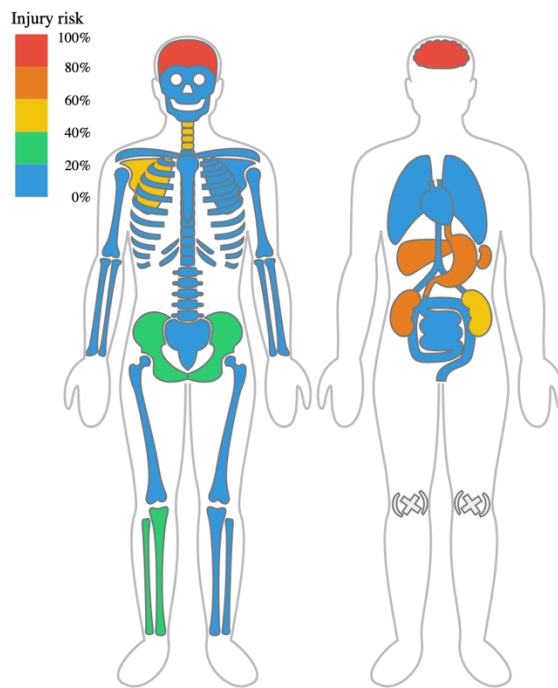


Figure 36 injury risk overview on the R-point impact

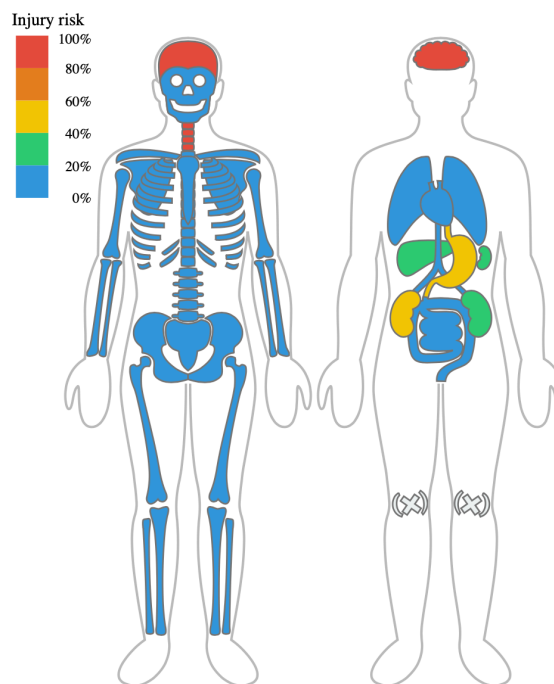


Figure 37 injury risk overview on rear impact

In both cases, 100%tile is considered. However, for the injury risk, all the risk curves are generated based on the Weibull distribution, introduced in chapter 2.4. However different criteria are adopted for different parts . For the bones and brain, MPS criteria were adopted. For the internal organs CSDM criteria are chosen. A complete data list can be seen in Table 6.

Bones	Brain	Organs
Maximum principal stress		CSDM
Weibull distribution (x is MPS or CSDM)		$P = 1 - e^{-(\frac{x}{a})^k}$
b=1		
a=0.0275	a=1.05	a=0.6162
k=3.013	k=2.84	k=1.8

Table 6 criteria and parameters adopted for different body parts

4.2 Energy balance

Energy balance is an indicator for assessing the success of the simulation, which considers six energy components such as:

- Total energy
- Kinetic energy
- Internal energy
- External energy
- Hourglass energy
- Sliding interface energy

Figures 38 and 39 show the energies plot for R-point impact and rear impact, respectively.

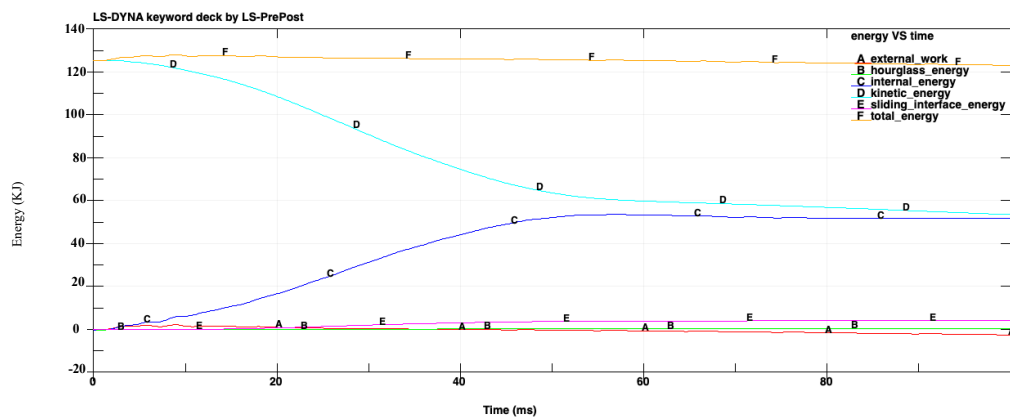


Figure 38 energy balance R-point impact

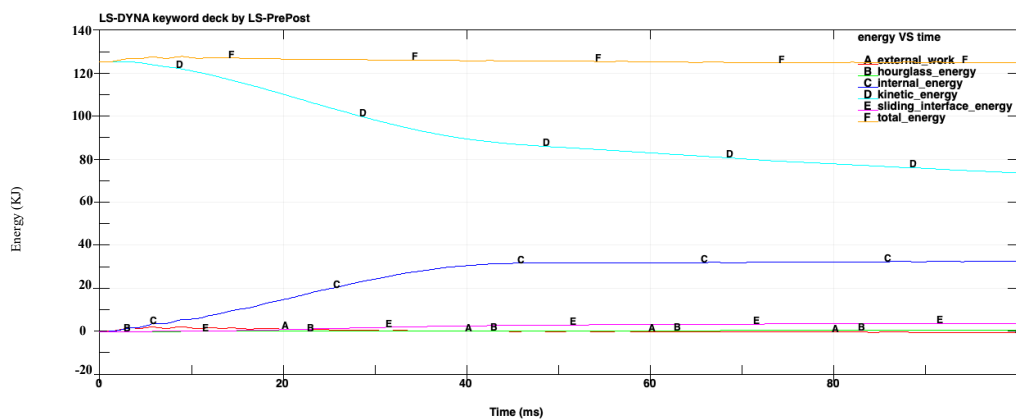


Figure 39 energy balance rear impact

Among these two simulations, it can be observed that slight variation exists in the total energy of both cases, they increase slightly after the simulation is initiated, and then decreases slowly. However, this level of variation is acceptable, considering the tiny probability of errors in the contacts of the model. As shown in the two figures, the trend of the kinetic energy and internal energy are correct. According to the Ls-Dyna guidelines about energy balance, the hourglass energy is a parameter that is correlated with the zero-energy mode of deformation that produces zero strain and no stress, it should be under 10% of the total energy, through both figures, constrain is satisfied. In the energy analysis, an important parameter that should be checked is the energy ratio, which is defined as follows:

$$e_{ratio} = \frac{E_{tot}}{E_{tot}^0 + W_{ext}} \quad (8)$$

Where:

E_{tot} = total energy

E_{tot}^0 = initial total energy

W_{ext} = external work

When the total energy equals the sum of the initial total energy and external work, then says the energy balance is perfect, which means the ratio should be close to one as possible to get a good simulation. In figures 40 and 41, the energy ratio for R-point impact and rear impact is presented. In both cases, the energy ratio varies during the time, but the difference is always controlled in 0.7%, for the R-point impact, in the last state, the energy ratio has around 0.15% variation, as for the rear impact it has higher variants, which is around 0.34%.

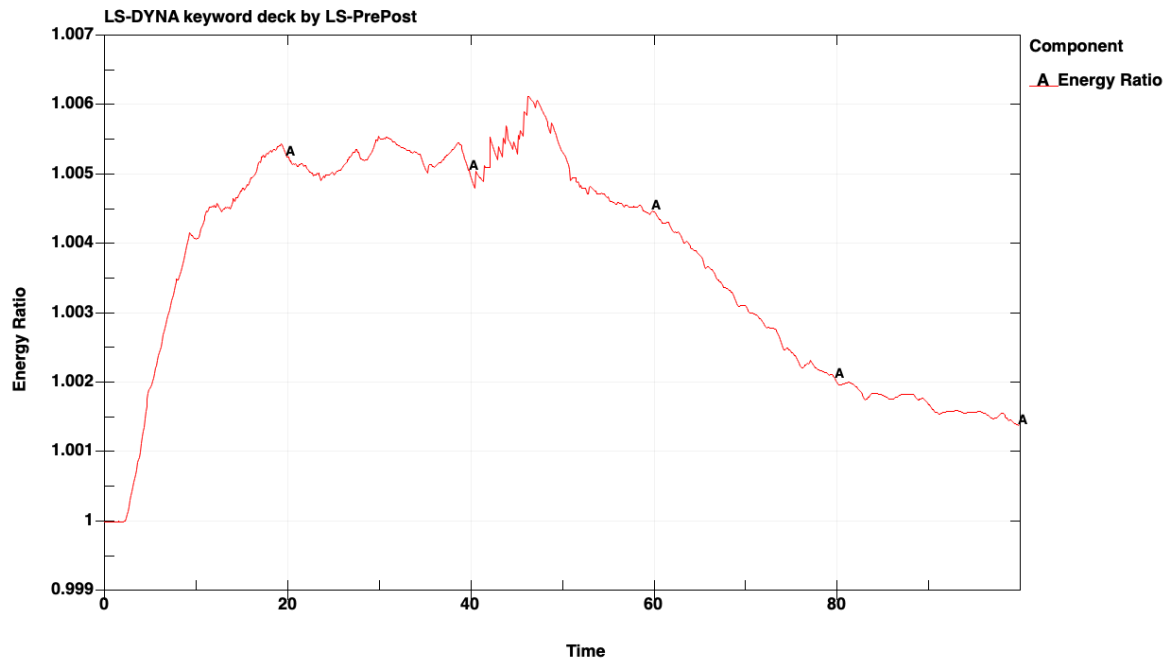


Figure 40 energy ratio for R-point impact

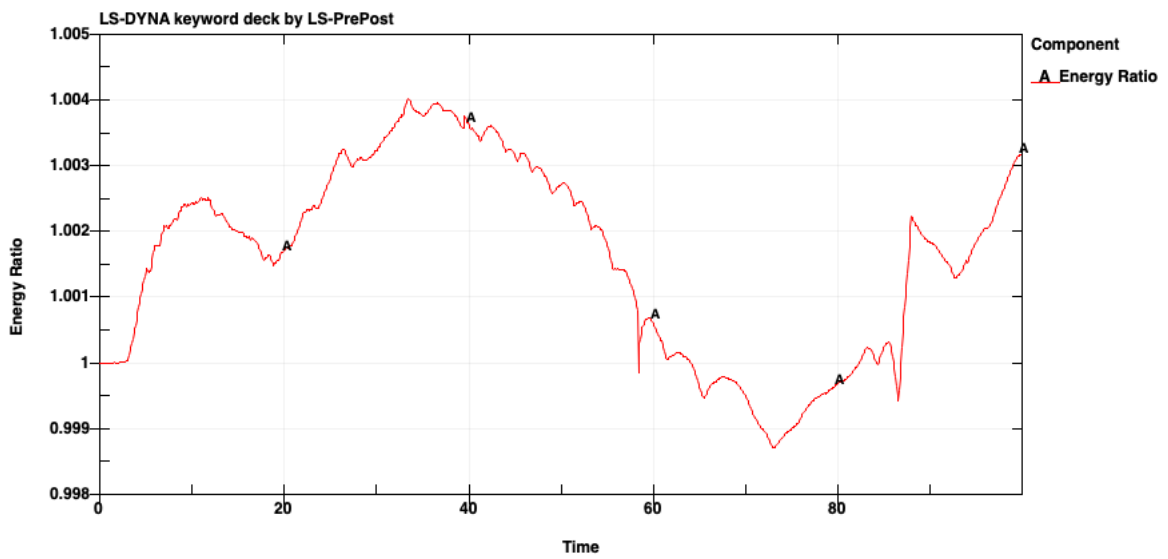


Figure 41 energy ratio for rear impact

4.2 Injury risk analysis in different impact scenarios

In this section, the injury risk results will be presented in different body regions, refereeing the figure 21. Among these regions, the injury risk, and the MPS data between the two cases will be compared and explained.

4.3.1 Injury risk analysis on the head

In the overview section, it can be observed that in both cases the head is one of the parts that suffer the most during the crush. In this section, the injury risks of three main parts will be introduced, including the brain, the skull, and the facial bone.

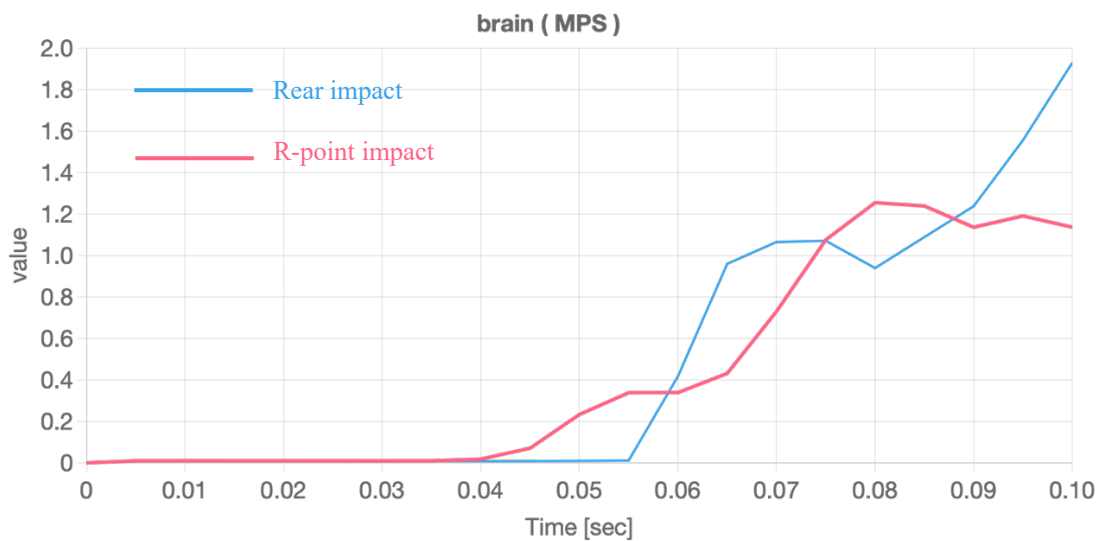


Figure 42 MPS log history of the brain on R-point impact (red) and rear impact(blue)

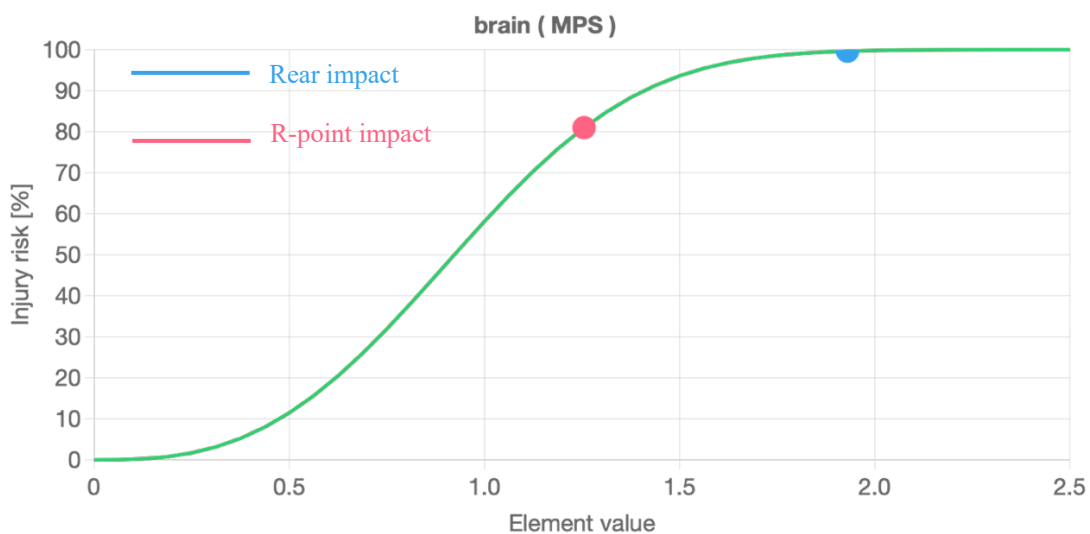


Figure 43 injury risk of the brain on R-point impact (red) and rear impact(blue)

From the figures above, during the rear impact, the brain suffers from higher MPS than the R-point impact, which is almost equal to 2. Referring to AIS 5+, which is a significant severe level of injury, the risk of getting injured by the rear impact is about 99.6%. As for the R-point impact, the MPS reaches the maximum value of about 1.26 at 8ms, which leads to 81% injury risk. It seems that compared to the R-point impact, the rear impact situation has a higher risk of injuring the brain. However, when considering the skull, as shown in figures 44 and 45, under the scenario of a rear impact, the MPS is only half of the R-point impact case, which are 0.035 and 0.8 respectively. The injury risk for the rear impact is 88.09%, and for the R-point impact is 100%.

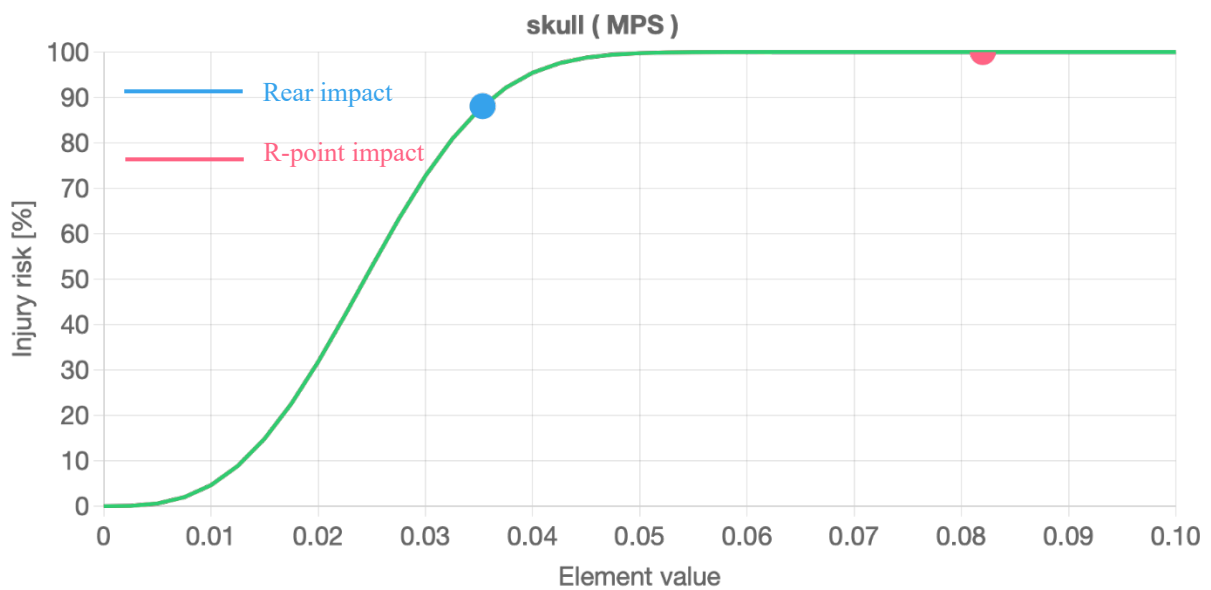


Figure 44 injury risk of the skull on R-point impact (red) and rear impact(blue)

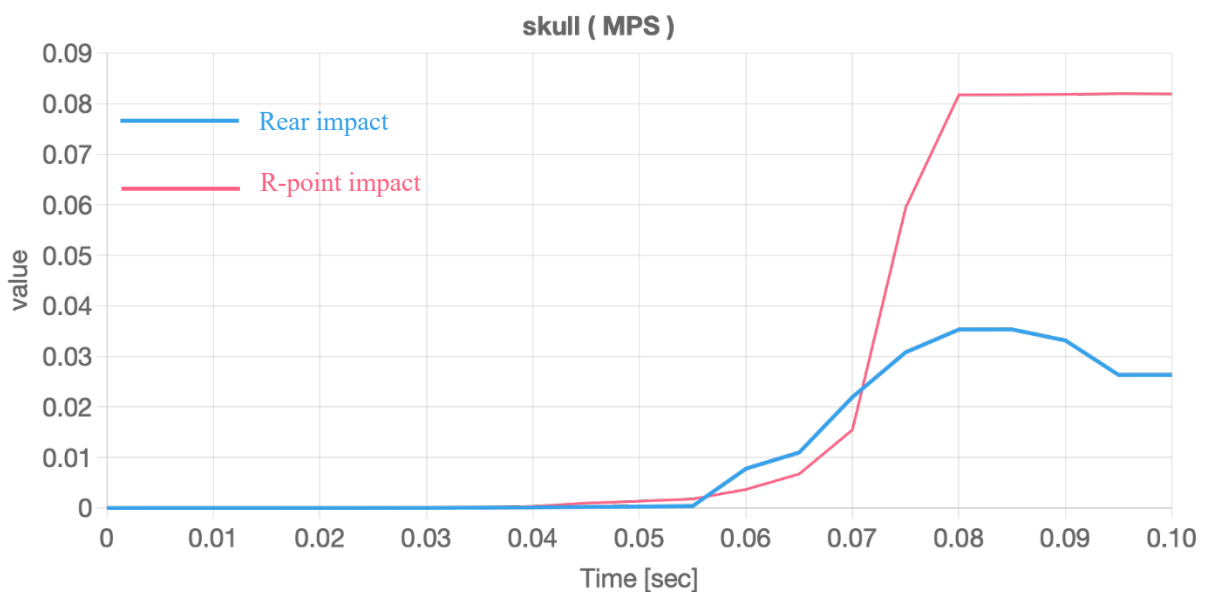


Figure 45 MPS log history of the skull on R-point impact (red) and rear impact(blue)

In both cases, the facial bone has a very low injury risk which is around 0.05% for the rear impact, and 0.02% for the R-point impact.

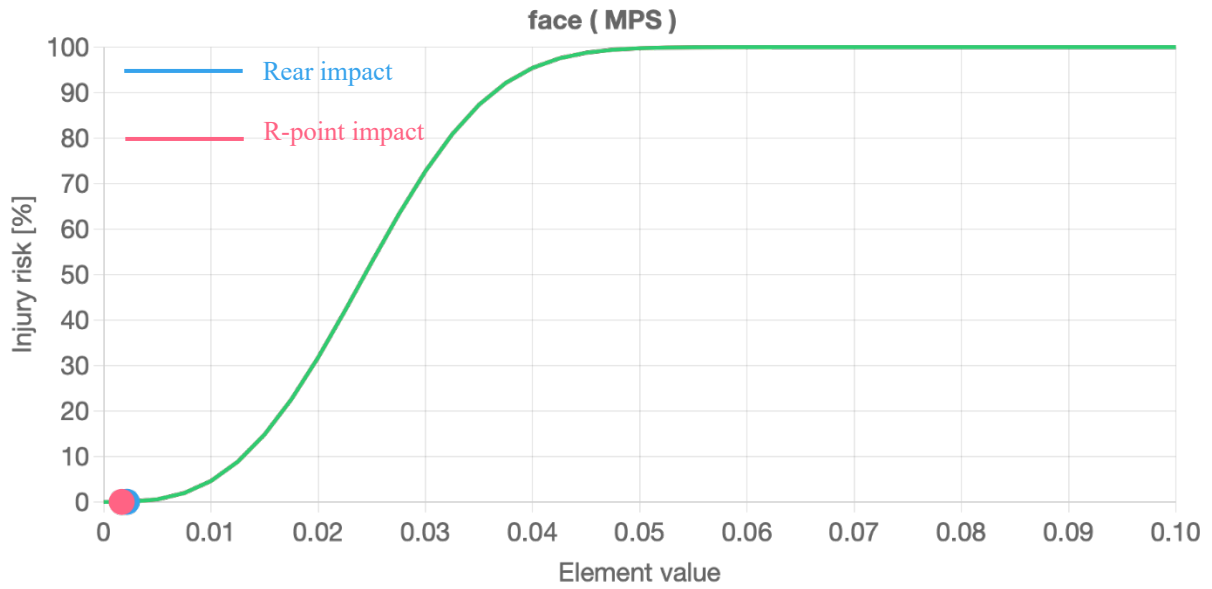


Figure 46 injury risk of the facial bone on R-point impact (red) and rear impact (blue)

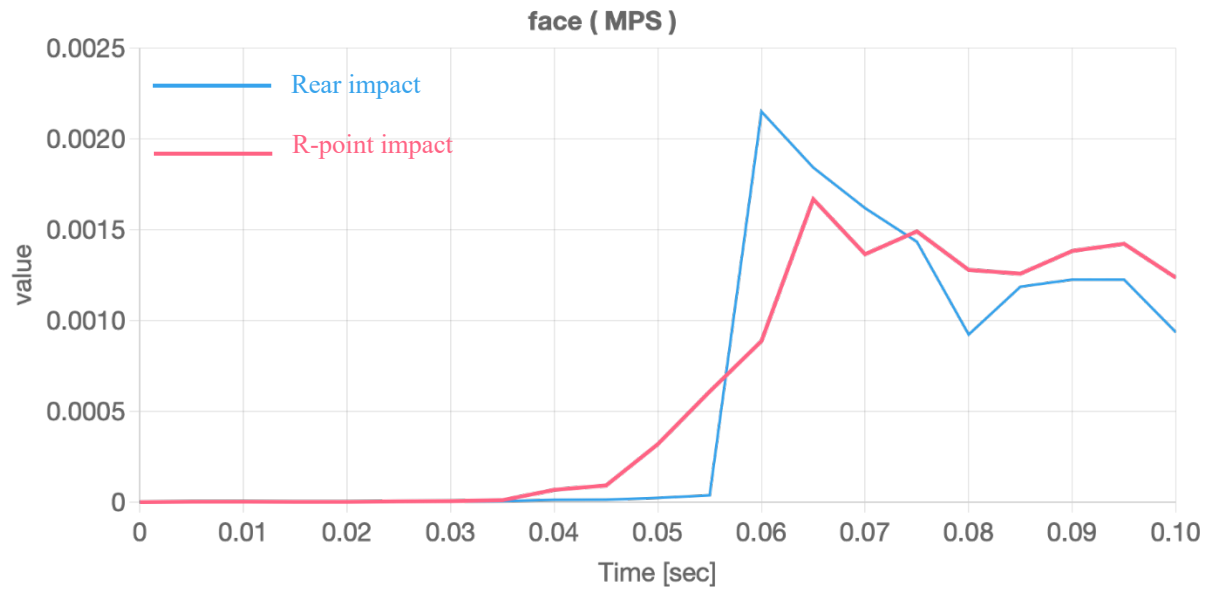


Figure 47 MPS log history of the facial bone on R-point impact (red) and rear impact (blue)

4.3.2 Injury risk analysis on the neck

The neck is also a significant part that should be analysed, observing the Figures in the [overview](#) sections, the cervical spines are stretched and extended during the crash. Especially for the rear impact case, due to higher momentum, its cervical spine suffers more than the R-point impact case. In Figure 48, after 6.5ms, the MPS value of the rear impact case increases rapidly and reaches the peak value of around 0.036, higher than the peak value of the R-point impact value which is about 0.023. This fact causes the rear impact to have a higher injury risk on the cervical spine than the R-point impact, which are 90.68% and 48.04% respectively.

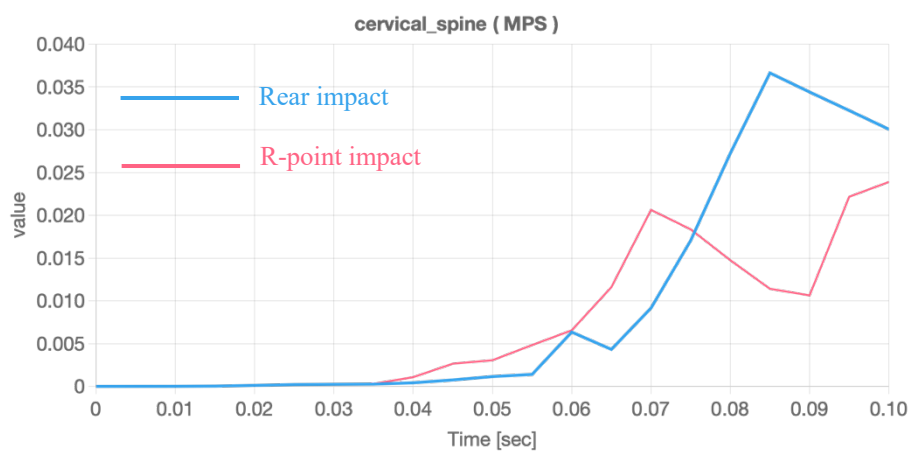


Figure 48 MPS log history of the cervical spine on R-point impact (red) and rear impact (blue)

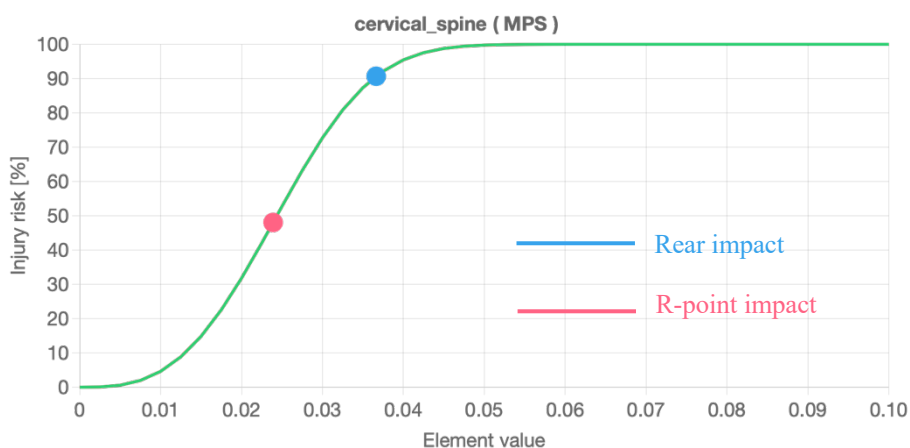


Figure 49 Injury risk of the cervical spine on R-point impact (red) and rear impact (blue)

4.3.3 Injury risk analysis on the Thorax

The thorax region contains the clavicle, the scapula, the ribs, the sternum, and the thoracic spine.

- The injury risk analysis on the clavicle

The clavicles on both sides in two cases are not experiencing a severe problem. As can be observed in the figures below, the injury risk in any case on both sides is below 1 %.

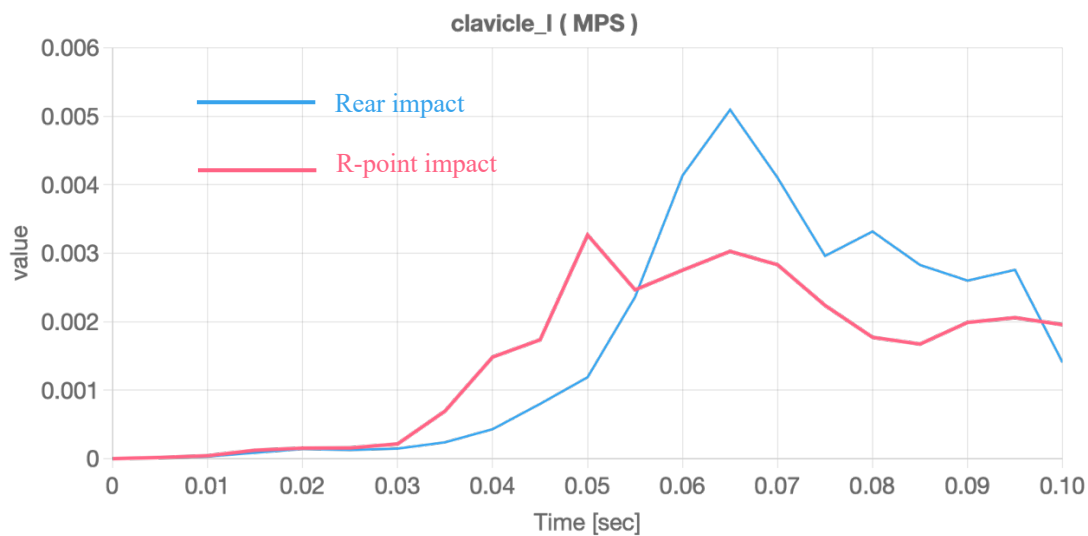


Figure 50 MPS log history of the left-side clavicle on R-point impact (red) and rear impact (blue)

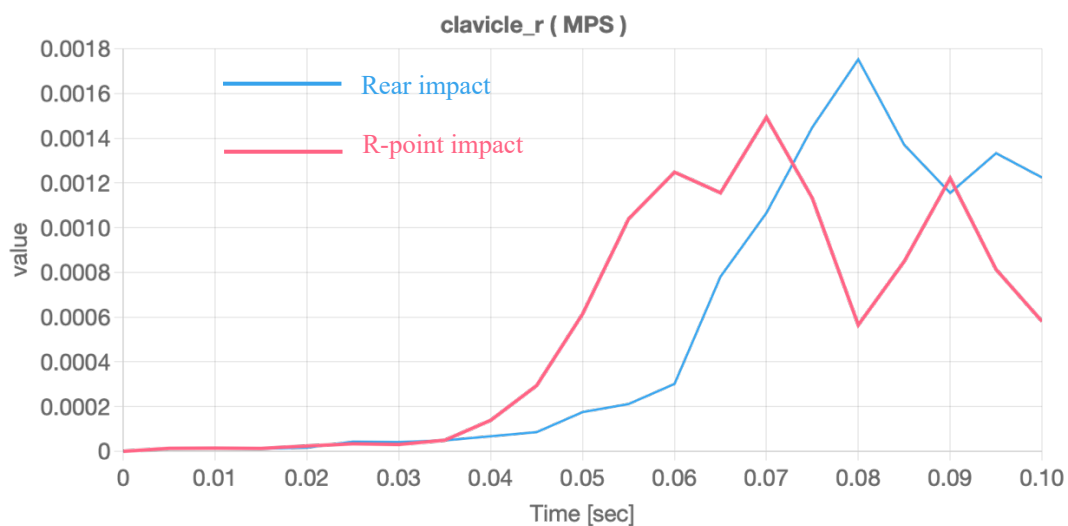


Figure 51 MPS log history of the right-side clavicle on R-point impact (red) and rear impact (blue)

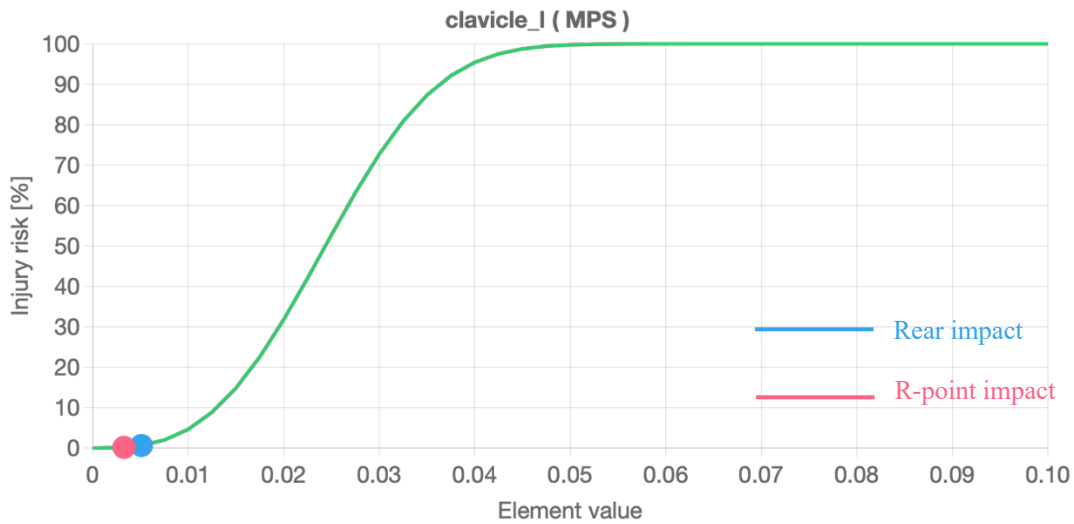


Figure 52 Injury risk of the left-side clavicle on R-point impact (red) and rear impact (blue)

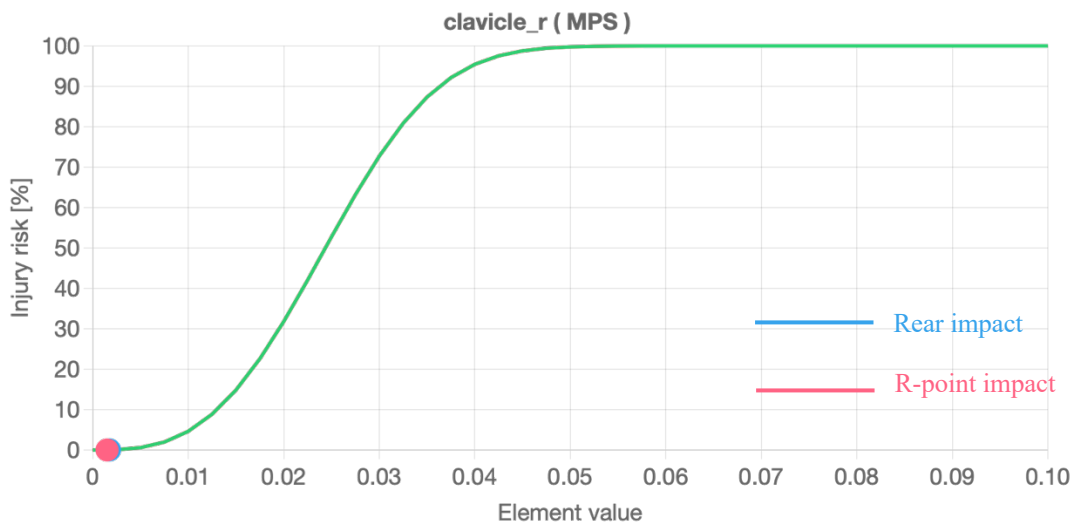


Figure 53 Injury risk of the left-side clavicle on R-point impact (red) and rear impact (blue)

- The injury risk analysis on the scapula

During the crash simulation, it is obvious that the one side of the scapula is impacted, from Figure 54, it can be seen that the right-side scapula of the R-point impact takes a high strain, because in this case, the impact position is extremely close to the human, the right-side scapula absorbs the force the directly from the impact, where the maximum principal strain is 0.0238, the injury risk can be calculated, which is 47.8% and relatively much higher than other cases. For the right-side rear impact, the injury risk is 2.33%. As for the left-side scapula, because there are no extra external forces applied to it directly, the MPS of it is very low in both cases, hence the injury risks for R-point impact and rear impact are 1.34% and 1.72% respectively.

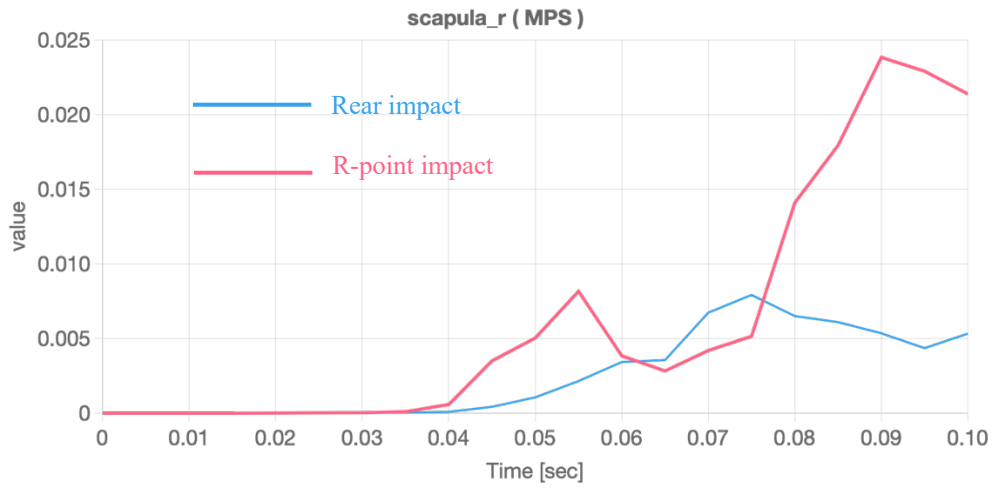


Figure 54 MPS log history of the right-side scapula on R-point impact (red) and rear impact (blue)

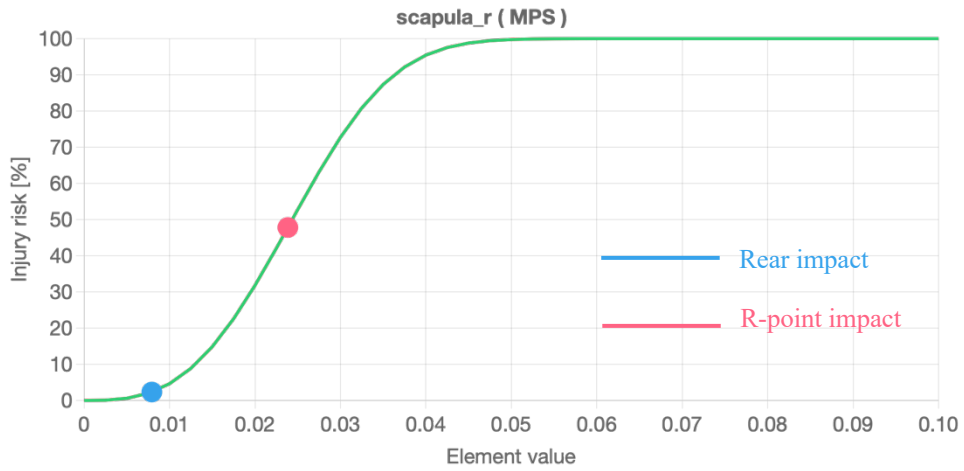


Figure 55 Injury risk of the right-side scapula on R-point impact (red) and rear impact (blue)

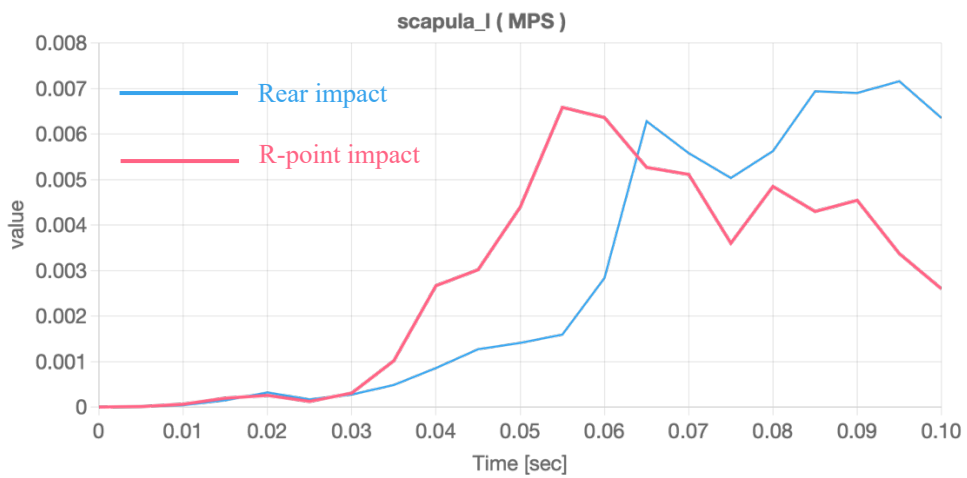


Figure 56 MPS log history of the left-side scapula on R-point impact (red) and rear impact (blue)

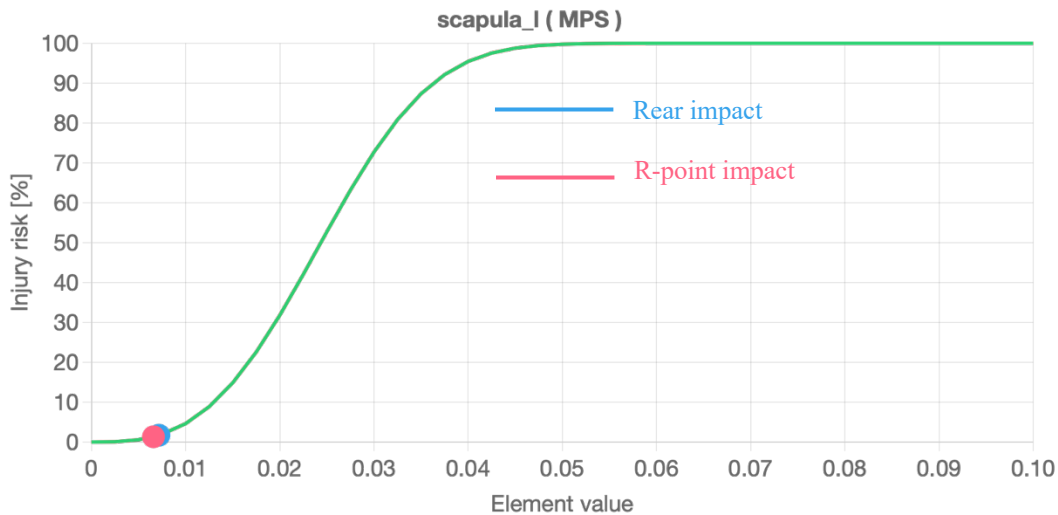


Figure 57 Injury risk of the left-side scapula on R-point impact (red) and rear impact (blue)

- The injury risk analysis on the Ribs

The analysis of the ribs can be on an overall evaluation for each simulation scenario or detailed on each rib between the left and right side, each side has 12 ribs, and the MPS on each rib is evaluated, same as the injury risk. Overall, in the two simulation scenarios, the most significant case is during the R-point impact, referring to AIS 2+, the injury risk of the ribs is 4.6%. A complete injury risk list from AIS0+ to AIS3+ of the ribs can be seen in Table 7 below. Analysing separately, according to the result, for both simulation cases, none of the ribs is experiencing severe damage. For R-point impact, the most deformed two ribs are the rib 11 on the left side with an injury risk of 6.63% and the rib 1 on the right side with an injury risk of 4.53%. For the rear impact, rib 1 is the most deformed rib on both sides with an injury risk of 0.08%. the Figures, and Table 8, below show detailed views about them.

INJURY RISK		
	R-point	Rear
AIS 0+	69,85%	92,97%
AIS 1+	30,15%	7,03%
AIS 2+	4,64%	0,23%
AIS 3+	0,44%	0,00%

Table 7 overall injury risk of the ribs on different AIS level

	R-point impact				Rear impact			
	left side		right side		left side		right side	
	MPS	injury risk	MPS	injury risk	MPS	injury risk	MPS	injury risk
rib1	0,004134	0,33%	0,009924	4,53%	0.005302	0,70%	0.002576	0,08%
rib2	0,002916	0,12%	0,004199	0,35%	0.002926	0,12%	0.001543	0,02%
rib3	0,006509	1,29%	0,004616	0,46%	0.006753	1,44%	0.001531	0,02%
rib4	0,005049	0,60%	0,004994	0,58%	0.004268	0,36%	0.002689	0,09%
rib5	0,006061	1,04%	0,008618	2,99%	0.005865	0,95%	0.004685	0,48%
rib6	0,004637	0,47%	0,009891	4,49%	0.004722	0,49%	0.004002	0,30%
rib7	0,006443	1,25%	0,007632	2,08%	0.003582	0,21%	0.002919	0,12%
rib8	0,006849	1,51%	0,006012	1,02%	0.003467	0,19%	0.002841	0,11%
rib9	0,007391	1,89%	0,002932	0,12%	0.003302	0,17%	0.001533	0,02%
rib10	0,008469	2,84%	0,003824	0,26%	0.006164	1,10%	0.003196	0,15%
rib11	0,011302	6,63%	0,001444	0,01%	0.002623	0,08%	0.001285	0,01%
rib 12	0,004418	0,40%	0,000882	0,00%	0.002205	0,05%	0.000764	0,00%

Table 8 injury risk on each rib for both scenarios

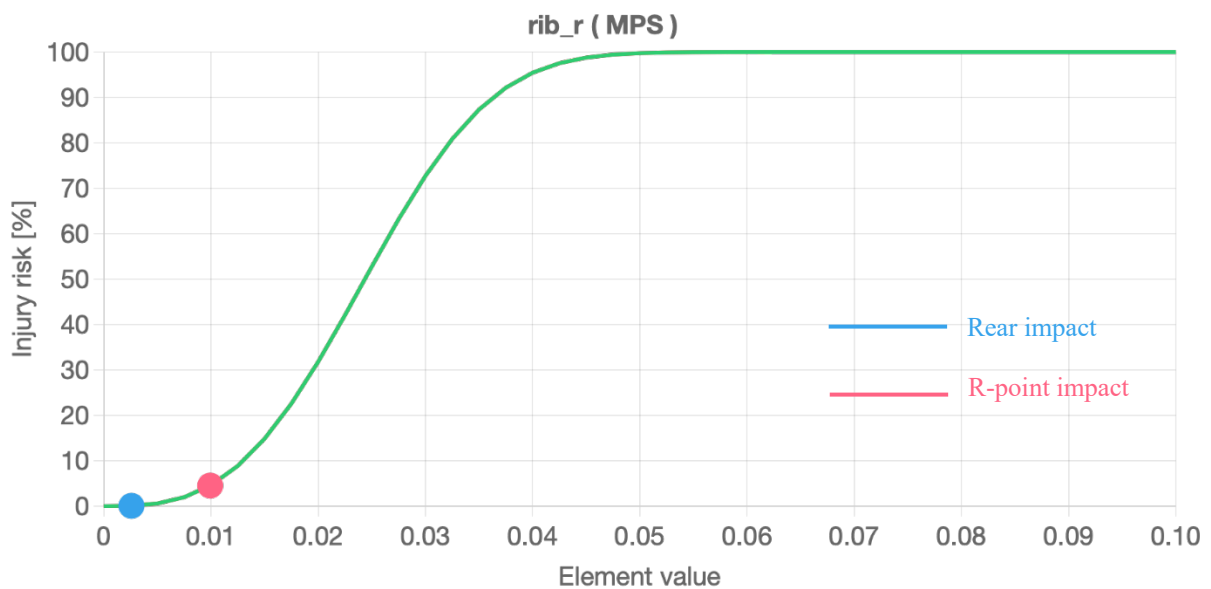


Figure 58 Maximum Injury risk of the right-side ribs on R-point impact (red) and rear impact (blue)

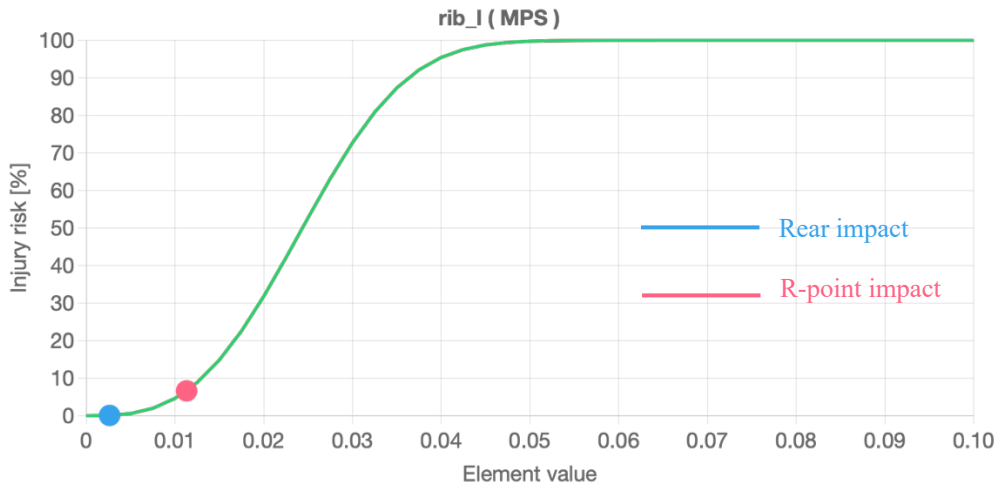


Figure 59 Maximum Injury risk of the left-side ribs on R-point impact (red) and rear impact (blue)

From Figures 60-62 in the R-point impact, the ribs start to deform after 3 ms, where the trolley impacts the vehicle and decreases during the last stage. However, for the rear impact, the ribs start deforming in the middle stage of the crash, and continue the increment, with slight attenuation in the last stage.

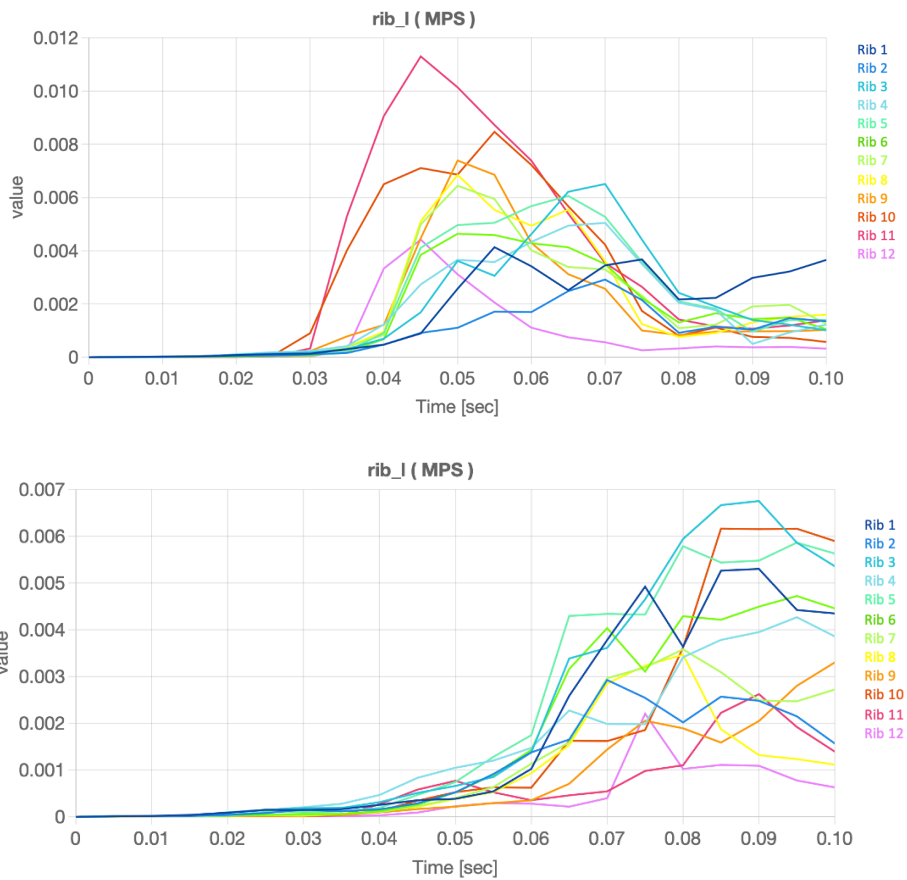


Figure 60 MPS log history of each rib on the left side of the R-point impact(upper) and rear impact (lower)

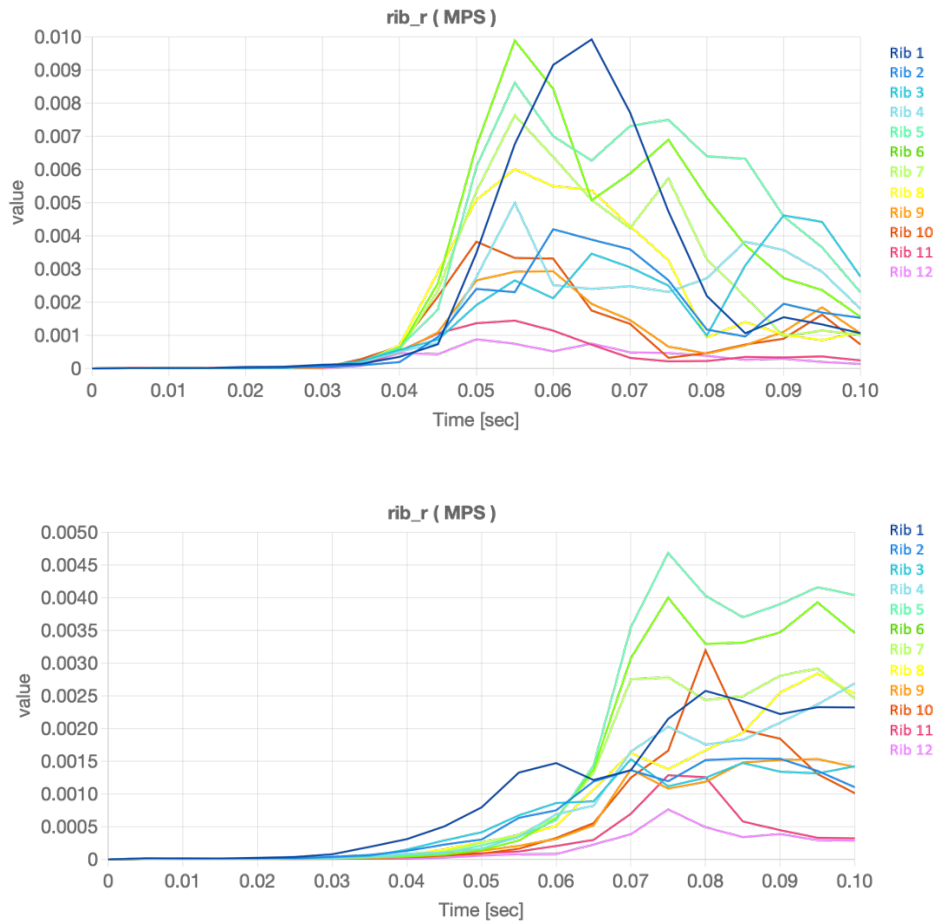


Figure 61 MPS log history of each rib on the right side of the R-point impact(upper) and rear impact (lower)

- The injury risk analysis on the sternum

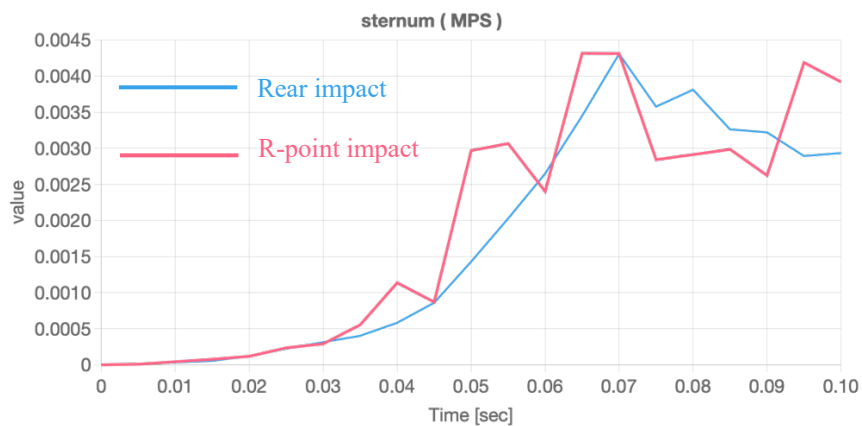


Figure 62 MPS log history of the sternum on the R-point impact (red) and the rear impact (blue)

From Figure 62, the MPS of the sternum in both cases reaches a peak value very similar at 7 ms, the value is 0.004315 for the R-point impact case and 0.004308 for the rear impact case,

with negligible differences, hence, they have the same injury risk, equal to 0.37% as shown in Figure 63.

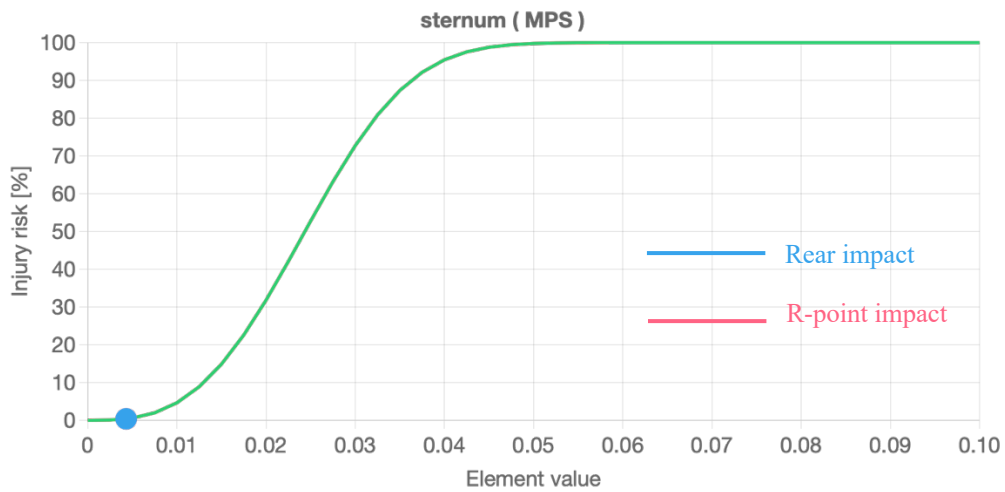


Figure 63 injury risk of the sternum

- The injury risk analysis on the thoracic spine

In the rear impact case, the thoracic spine has a similar situation to the sternum, with the MPS around 0.007. On the other hand, the R-point impact has a higher value, around 0.01, but still not a severe case, in both cases, the injury risks are under 10%. The former is 1.71%, and the latter is 5.49%.

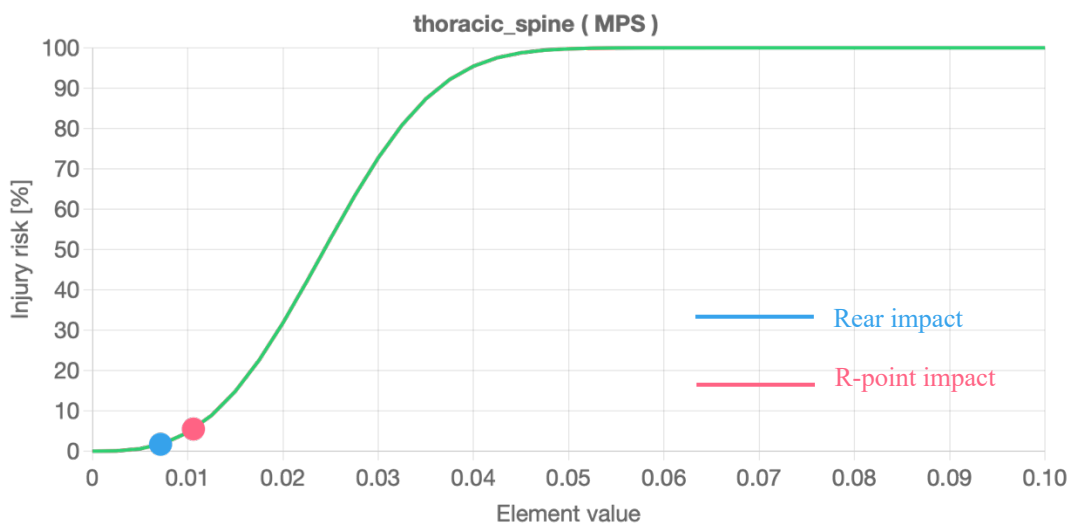


Figure 64 Injury risk of the thoracic spine on the R-point impact (red) and the rear impact (blue)

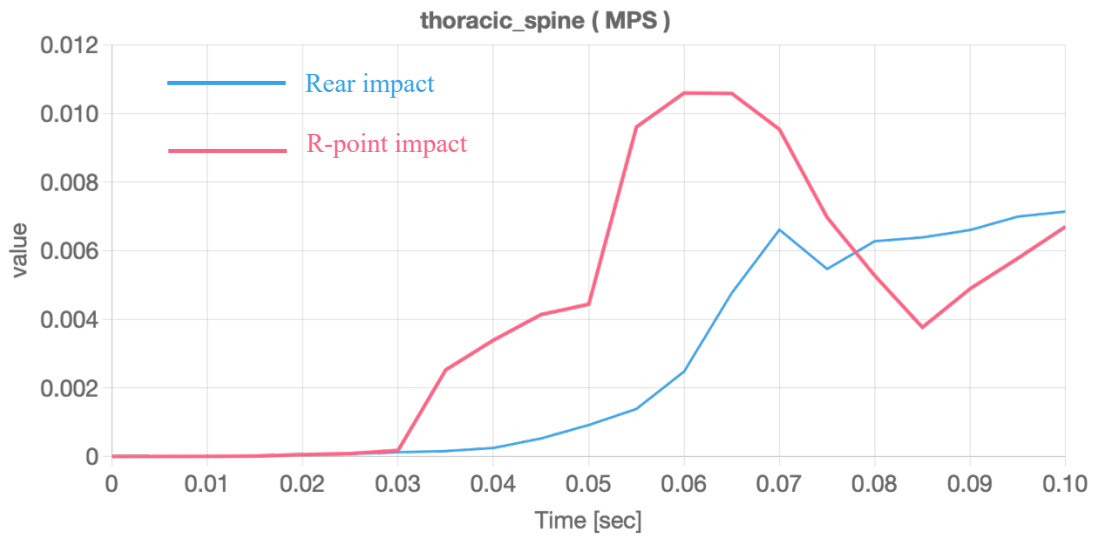


Figure 65 MPS log history of the thoracic spine on the R-point impact (red) and the rear impact (blue)

4.3.4 Injury risk analysis on the abdomen and pelvis

This body region includes three parts, the pelvis, the sacrum, and the lumbar spine.

- The injury risk analysis on the pelvis

According to the crash simulation, especially in the R-point impact scenario, the pelvis is a direct part of being impacted. Through Figures 66 and 67, for the R-point impact case, the deformation of the pelvis increases rapidly on both sides when the trolley starts the contact with the vehicle at 3 ms. Since the right side is closer to the trolley, the change is sharper than the left side, and at 5.5 ms, they reached a similar peak value of about 0.0191 on the right and 0.0197 on the left, with an injury risk of 28.96% and 31.82% respectively. As for the rear impact, both sides' pelvis was not having large deformation, the injury risk is much lower than in the other case, which is around 0.04% on the left and 0.09% on the right. As shown in Figures 68 and 69.

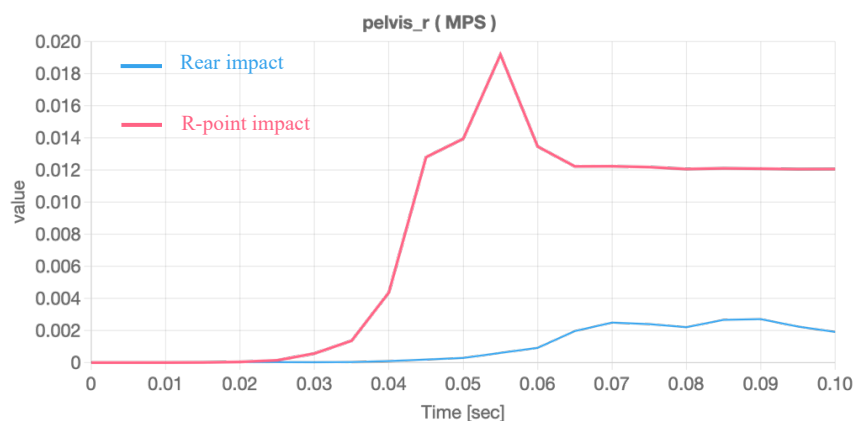


Figure 66 MPS log history of the right side pelvis on the R-point impact (red) and the rear impact (blue)

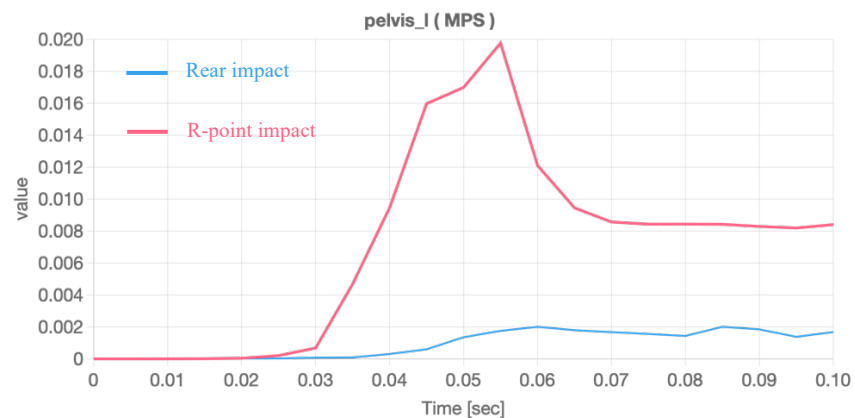


Figure 67 MPS log history of the left side pelvis on the R-point impact (red) and the rear impact (blue)

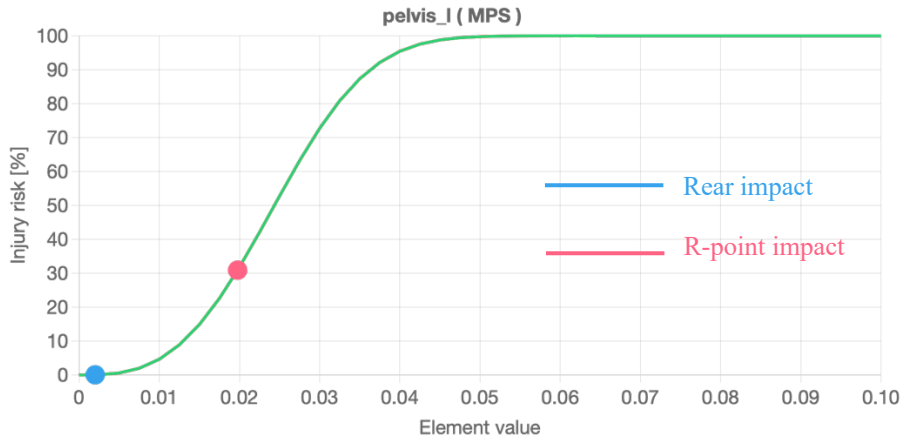


Figure 68 Injury risk of the left side pelvis on the R-point impact (red) and the rear impact (blue)

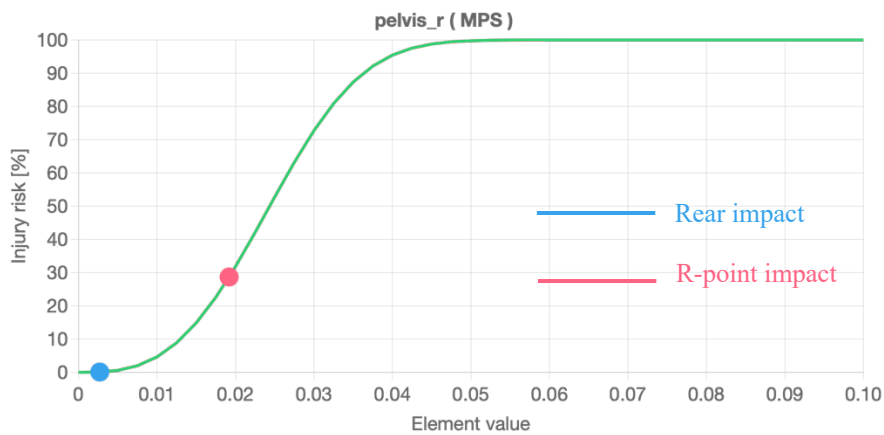


Figure 69 Injury risk of the right-side pelvis on the R-point impact (red) and the rear impact (blue)

- The injury risk analysis on the sacrum

The sacrum in both cases is in a very safe situation, the deformation is not obvious, and the injury risk in both scenarios is lower than 0.1%, for R-point impact, the injury risk is 0.03%, and the rear impact case is even lower, which is 0.01%.

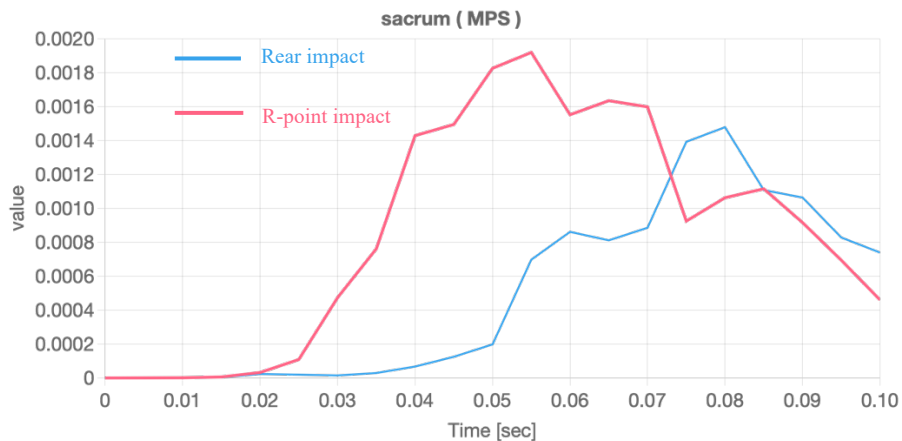


Figure 70 MPS log history of the sacrum on the R-point impact (red) and the rear impact (blue)

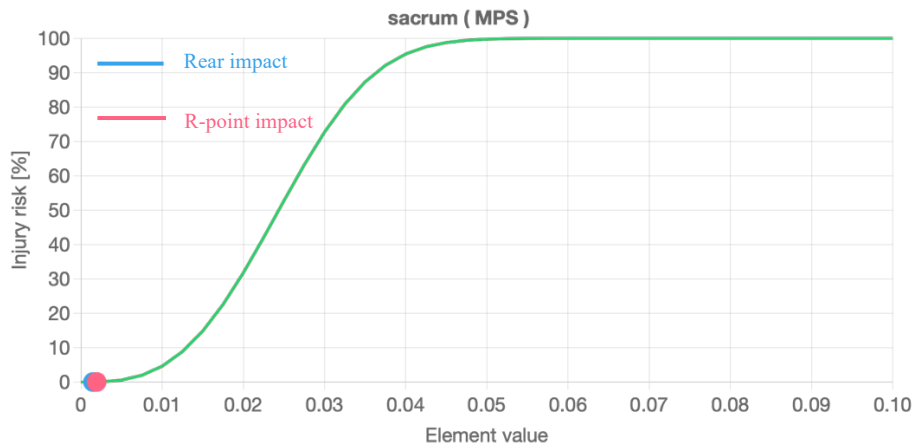


Figure 71 Injury risk of the sacrum on the R-point impact (red) and the rear impact (blue)

- The injury risk analysis on the lumbar spine

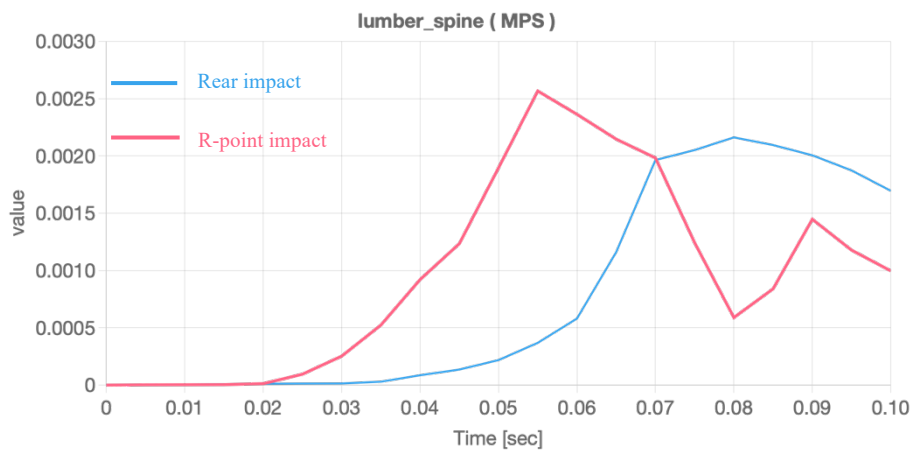


Figure 72 MPS log history of the lumbar spine on the R-point impact (red) and the rear impact (blue)

Figure 72 shows the deformation of the lumbar spine increases when the impact starts, they reach the peak value when the body has the closest contact with the vehicle and decrease after.

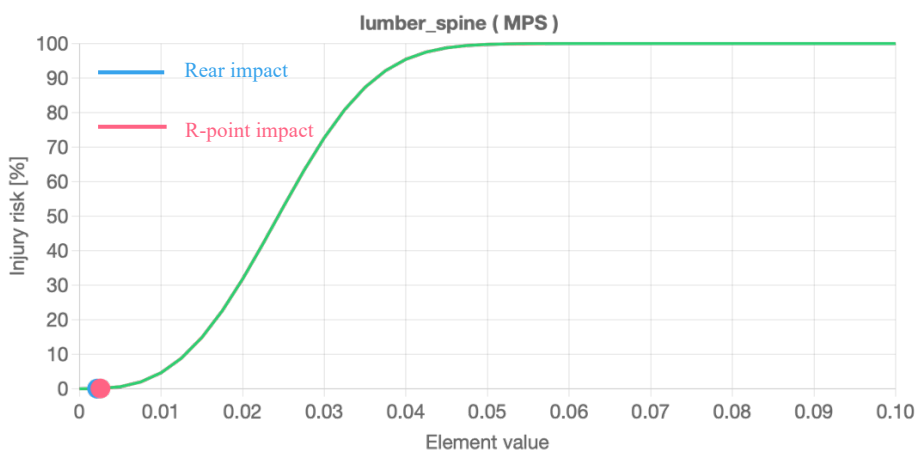


Figure 73 Injury risk of the lumbar spine on the R-point impact (red) and the rear impact (blue)

Both scenarios have similar values but are not significant in the number. The injury risks of the R-point and rear impacts are 0.08% and 0.05% respectively.

4.3.4 Injury risk analysis on the upper extremity

Four bones will be analysed in this section, the left and right side's humerus, and the left and right side's forearm. In both simulations, these two bones on the left and right sides are not at high risk of getting injured. The maximum MPS among them is in the R-point impact case on the right-side humerus, which is 0.009, and corresponding the highest injury risk is 3.11%. This situation could be due to the position of the human model, while the crash occurs, the driver's hands are on the steering wheel, and they are not being impacted by the stiff components of the cockpit directly, hence the risk of getting the bone on the upper extremity injured is reduced. The detailed data can be observed in the figures 74

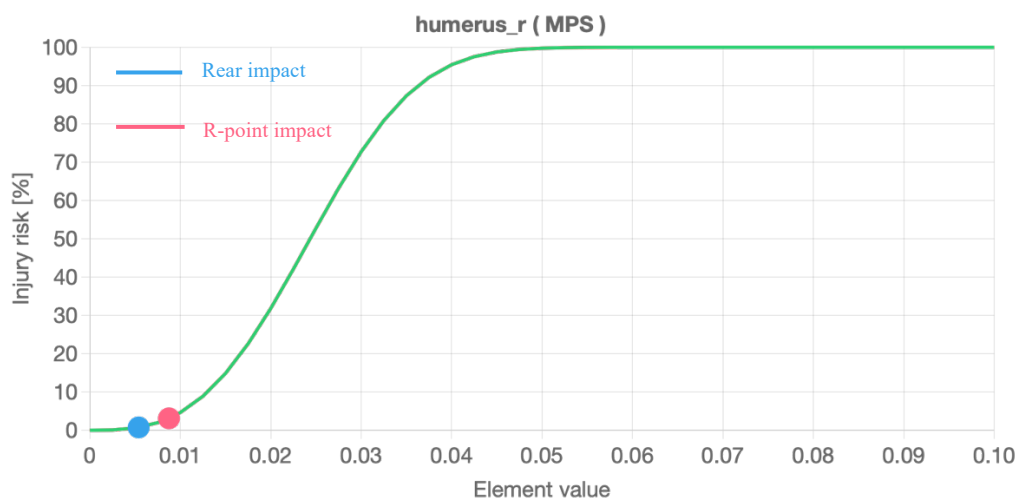


Figure 74 Injury risk of the humerus on the R-point impact (red) and the rear impact (blue)

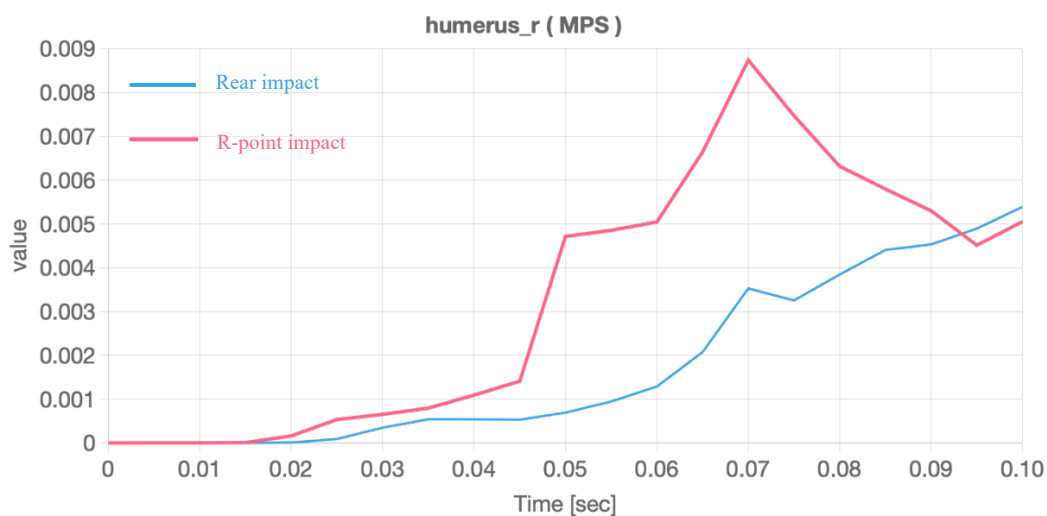


Figure 75 MPS log history of the humerus on the R-point impact (red) and the rear impact (blue)

4.3.4 Injury risk analysis on the lower extremity

Like the upper extremity, four bones are analysed for the lower extremity, including the left and right side's femur and the bone on the left and right side's leg. The lower extremity has a more critical situation than the upper extremity. Meanwhile comparing to the left side, the right-side leg has a more severe situation, which is closer to the door while the crash happens, the deformed door will have a straightforward contact with the right-side leg, especially for the R-point impact, the trolley is set extremely close to the HBM, the higher impact effect is expected, as shown in Figure 76. In the R-point impact, after the impact occurs, the deformed door presses the right leg, and with the elapsing of the time the deformation of the door increases, and the press to the leg increases, which leads to the deformation of the bone increase. Until the last stage, the deformation occurs a slight decrease, but only with a tiny difference between the peak value of 0.018. However, for the rear impact, during the crash, the frontal side of the vehicle was not deformed, what occurs on the lower leg, in this case, could be simply hit to the door by inertial, it is far lighter. The injury risk on the right-side lower leg for R-point impact is 24.52% and for the rear impact is 0.7%, as shown in Figure 77. This is the most significant case among these four bones.

For the rest of the three bones, the injury risks are under 2%, and the maximum injury risk among them is the lower leg of the left side, in the R-point impact case, the injury risk is about 1.72%

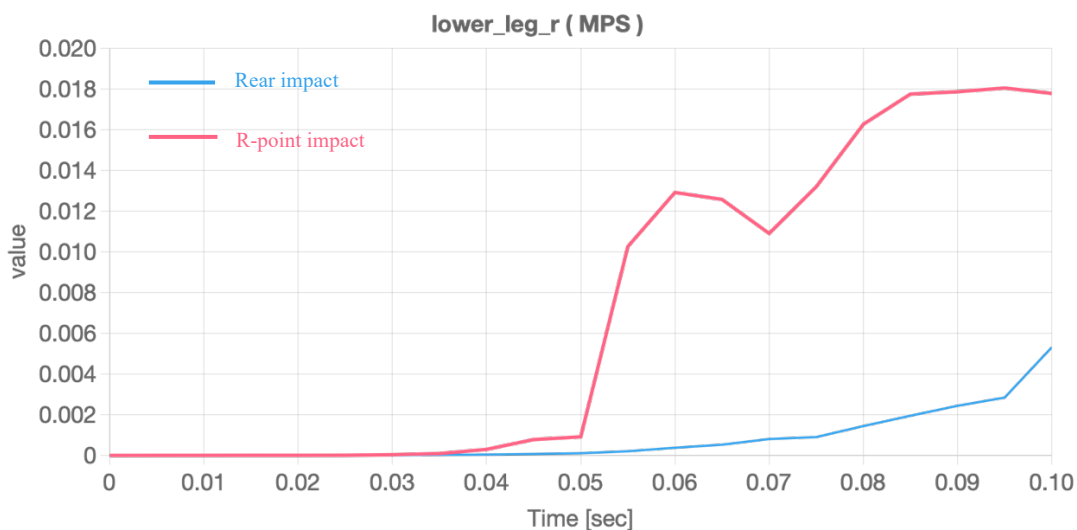


Figure 76 MPS log history of the right-side lower leg on the R-point impact (red) and the rear impact (blue)

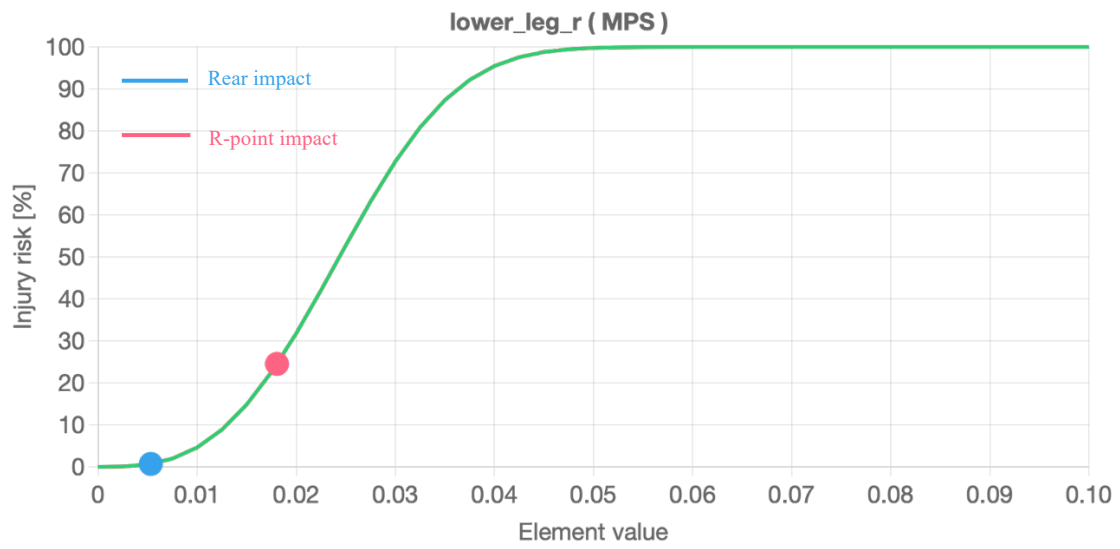


Figure 77 Injury risk of the right-side lower leg on the R-point impact (red) and the rear impact (blue)

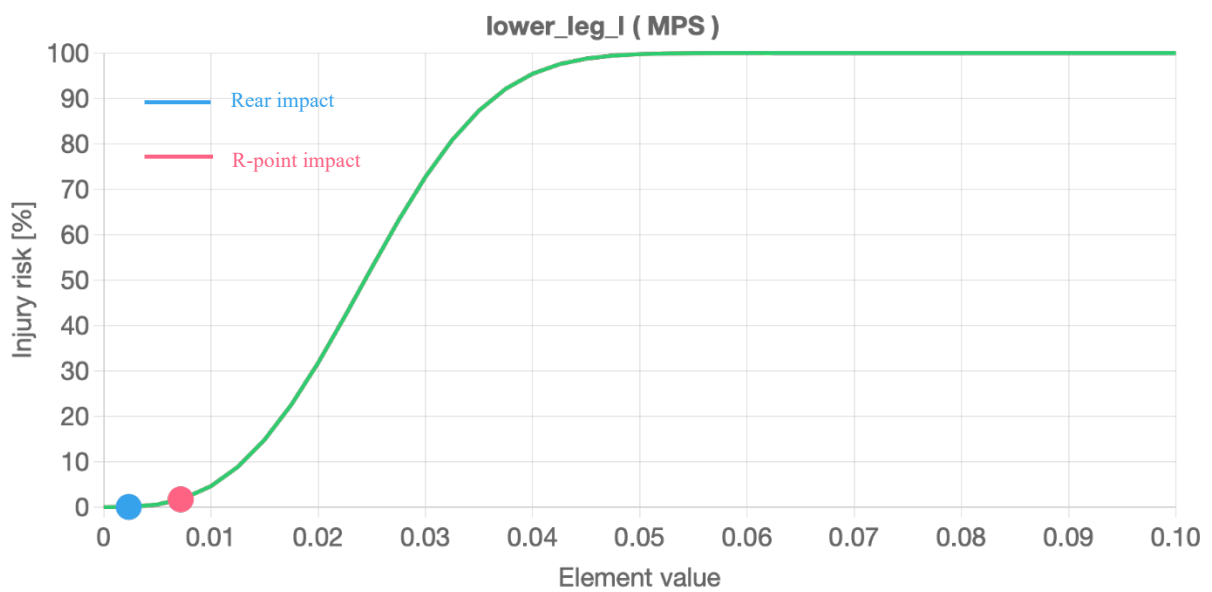


Figure 78 Injury risk of the left-side lower leg on the R-point impact (red) and the rear impact (blue)

4.3.4 Injury risk analysis on the internal organs

The internal organs being analysed are the heart, the left and right lung, the liver, the aorta, the spleen, the stomach, and the left and right-side kidney. Different from the other part of the body, in which the MPS was used to calculate the injury risk, the injury risks of the internal organs were estimated based on the CSDM (cumulative strain damage measurement), a measure of injury, which is based on the volume fraction of the internal organs that exceeds a given maximum principal strain threshold, and it is calculated by the application.

- Injury risk analysis of the heart

Unfortunately, because the application is under development for the region of the internal organ, bugs exist, and the injury risk curve and value of the heart were not able to be calculated automatically. But the CSDM value was estimated, as shown in Figure 79. The peak value for the R-point impact is higher than the rear impact, they all reach the peak at the last stage, which is 0.683 and 0.63 respectively.

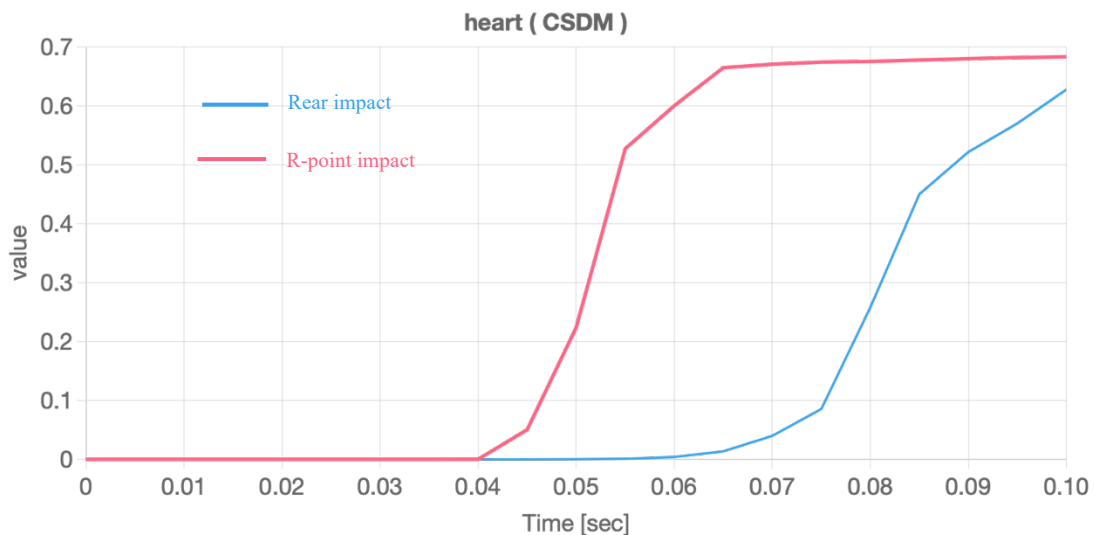


Figure 79 CSDM value of the heart along time on the R-point impact (red) and the rear impact (blue)

Applying Formula (6), the injury risk value is estimated. With the R-point impact, the heart has an injury risk of 57.11%, and with the rear impact, the heart has an injury risk of 52.56%

- Injury risk analysis of the lung

The lung has an analogical situation to the heart, the injury risk is not calculated, only the CSDM value is evaluated for both sides of the lung. As shown in Figures 80 and 81.

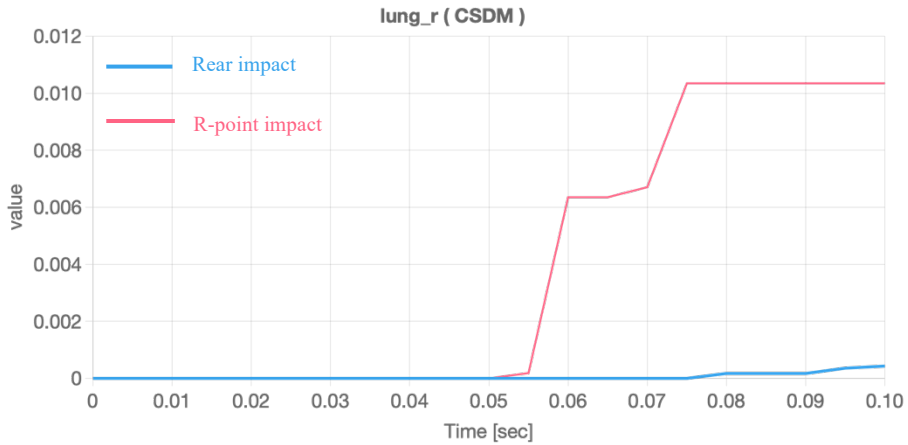


Figure 80 CSDM value of the right-side lung along time on the R-point impact (red) and the rear impact (blue)

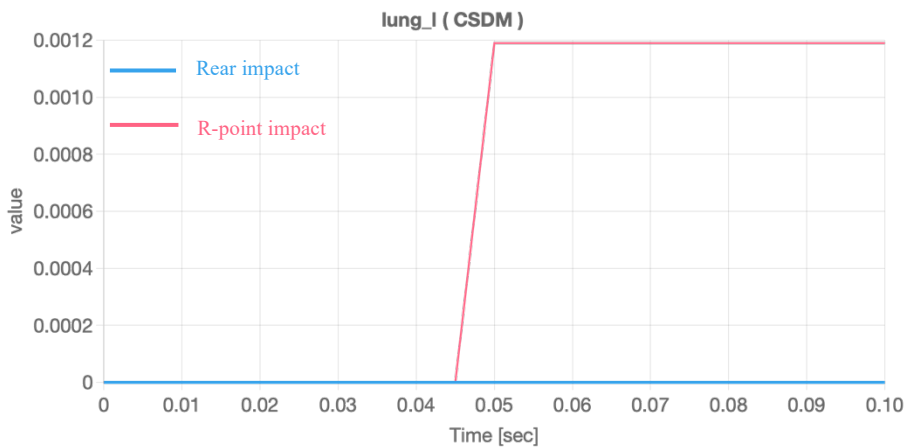


Figure 81 CSDM value of the left side lung along time on the R-point impact (red) and the rear impact (blue)

In the case of the rear impact, the lung's CSDM value can be neglected, the relatively significant case in the R-point impact is the right side's lung, the CSDM is about 0.01, but still would cause any injury, the risk is under 0.1%.

- Injury risk analysis of the liver

Compared to the rear impact case, the liver in the R-point impact has higher CSDM, around two times, which means the injury risk will be accordingly higher. Figure 83 shows that the injury risk is 69.77% for the R-point impact and rear impact with an injury risk of 25.32%.

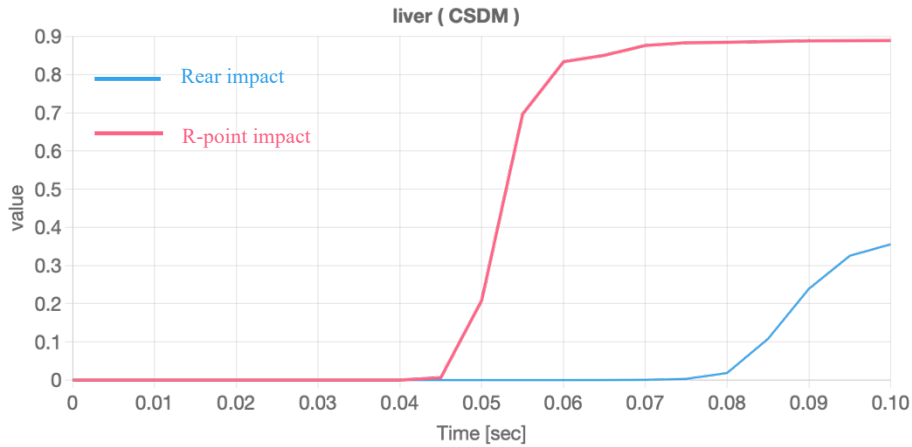


Figure 82 CSDM value of the liver along time on the R-point impact (red) and the rear impact (blue)

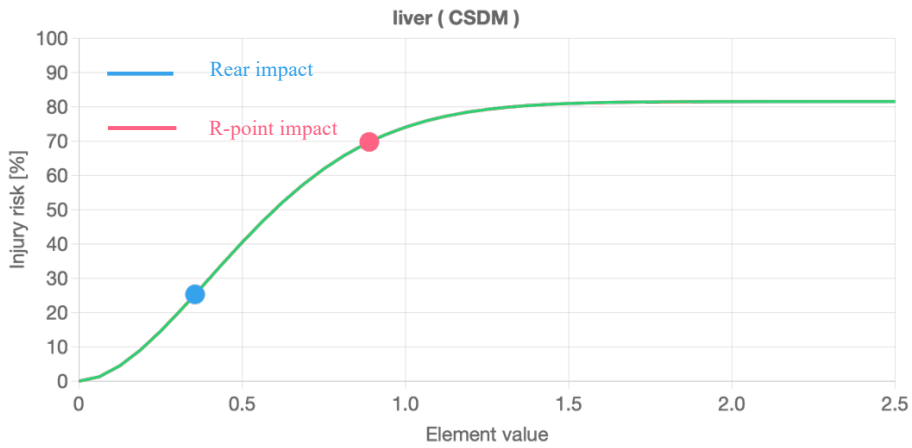


Figure 83 Injury risk of the liver on the R-point impact (red) and the rear impact (blue)

- Injury analysis of the spleen

The spleen has a slightly better situation than the liver, it is on the left side of the body with a small volume, during the crash it will be less impacted, but still, as a fragile organ, the effect from the impact cannot be neglected. The CSDM value in the R-point impact is higher than the rear impact as expected, they both reach the maximum value at the last phase, which is 0.751 and 0.442 respectively and the injury risk is 61.98% for the R-point impact, 34.46% for the rear impact.

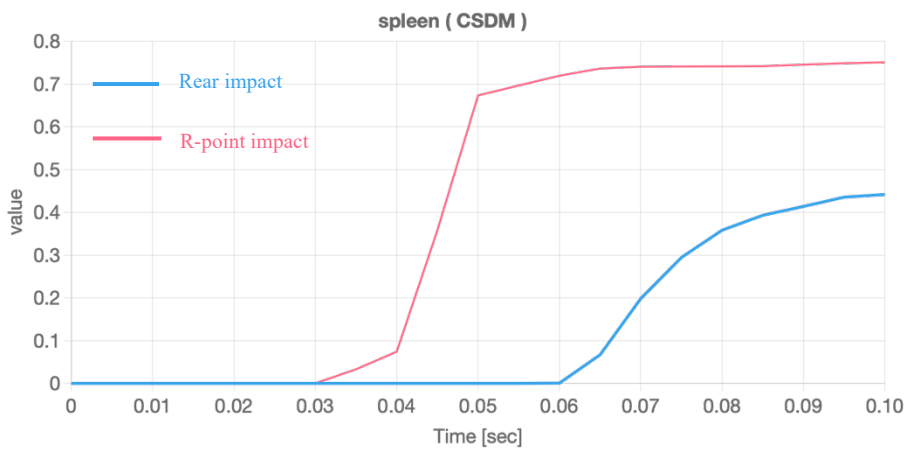


Figure 84 CSDM value of the liver along time on the R-point impact (red) and the rear impact (blue)

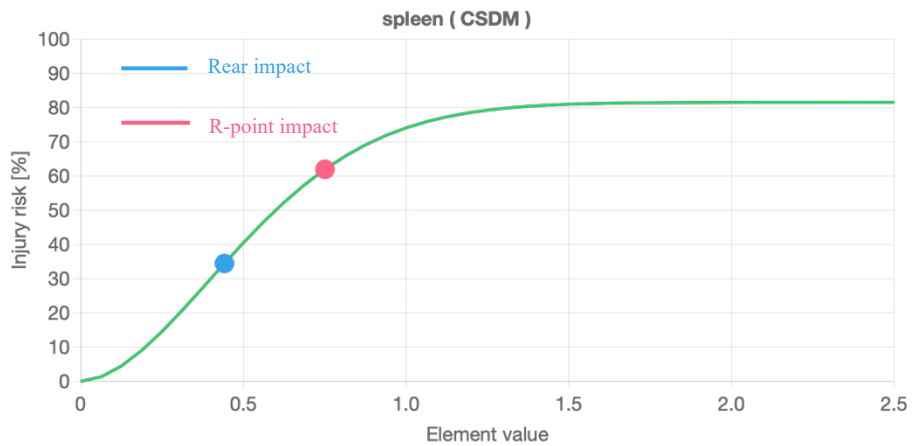


Figure 85 Injury risk value of the spleen on the R-point impact (red) and the rear impact (blue)

- Injury analysis of the stomach

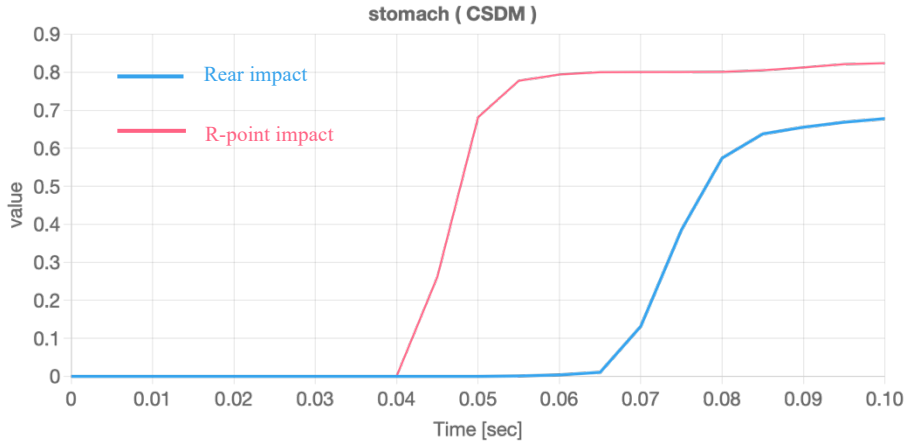


Figure 86 CSDM value of the stomach along time on the R-point impact (red) and the rear impact (blue)

In both cases, the stomach seems at high risk of injury, and the CSDM value of the rear impact is close to the R-point impact but with a lower value, which is the same as the injury risk. For the stomach in the R-point impact, the injury risk is 66.45% and 56.68% for the rear impact simulation.

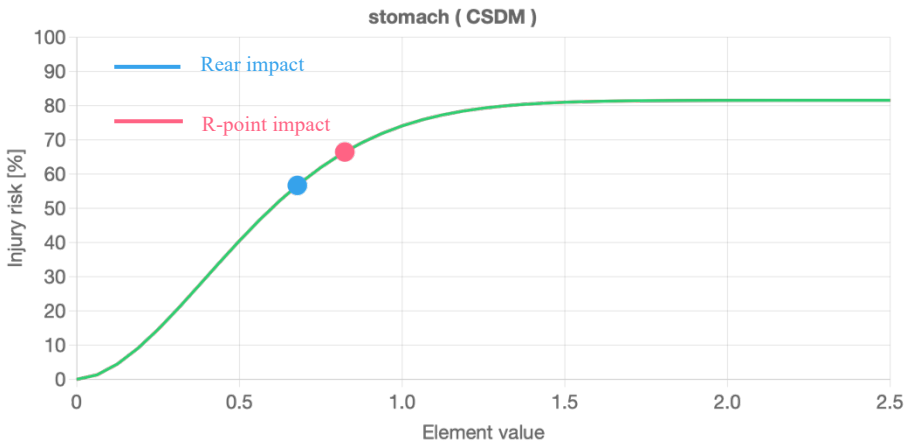


Figure 87 Injury risk value of the stomach on the R-point impact (red) and the rear impact (blue)

- Injury analysis of the kidney

among all the organs being analysed, the kidney has the highest injury risk in all the scenarios being simulated in this thesis. Especially the right-side kidney in the R-point impact case, with the CSDM value of 0.94, the injury risk is up to 71.81%, compared to it, the left side is lower, which is about 52.84%. While in the rear impact case, the situation is better, the injury risk on the left side is 37.9%, and on the right side is 44.5%.

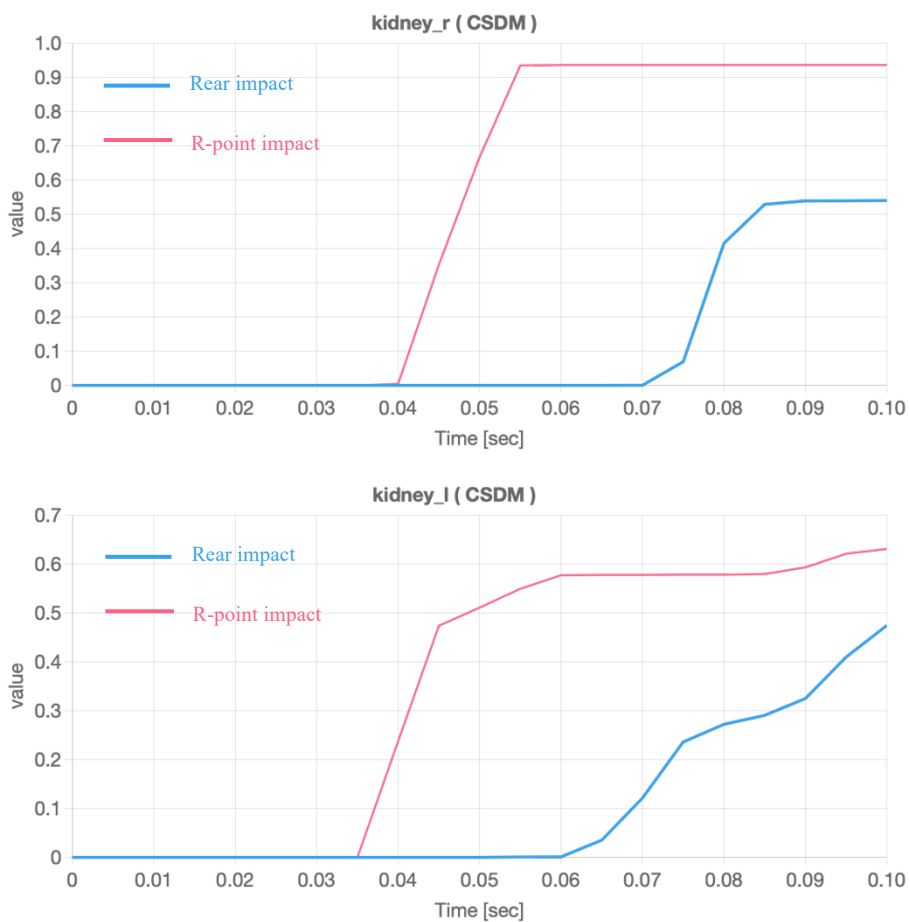


Figure 88 CSDM value of the left-side(lower) and right-side(upper)kidney on the R-point impact (red) and the rear impact (blue)

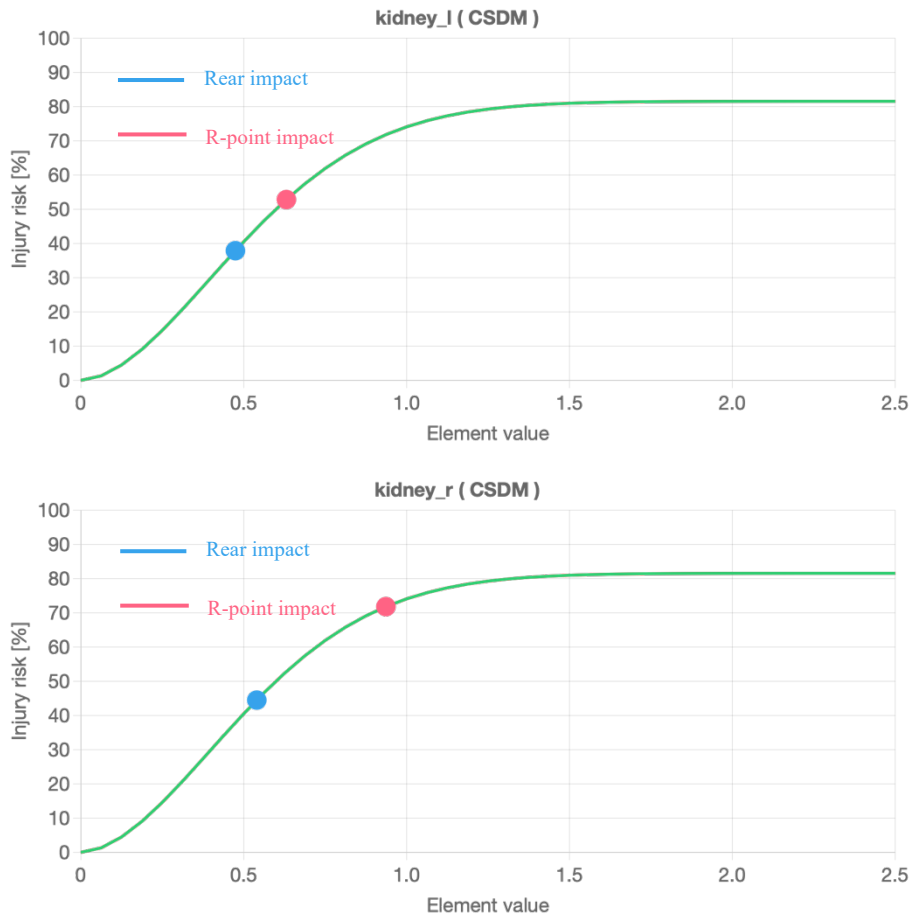


Figure 89 Injury risk of the left-side(lower) and right-side(upper)kidney on the R-point impact (red) and the rear impact (blue)

- Injury analysis of the intestine

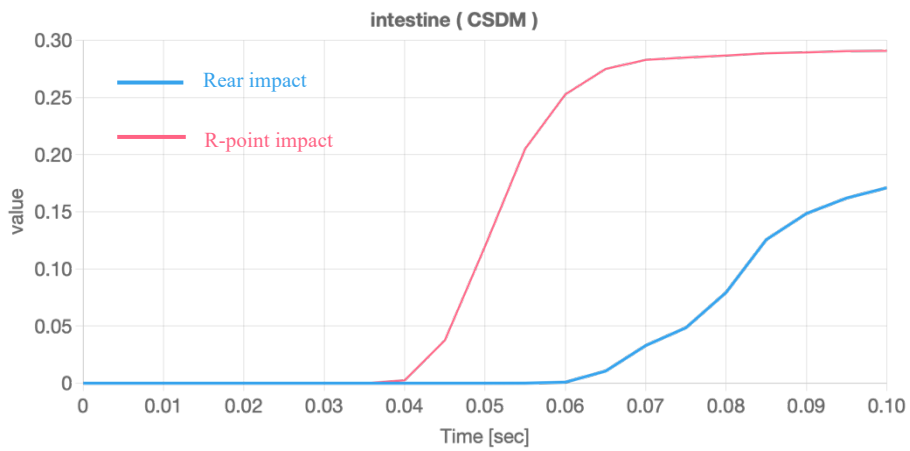


Figure 90 CSDM value of the intestine along time on the R-point impact (red) and the rear impact (blue)

The intestine does not have a high value of the CSDM in both cases, the maximum number

that they reach is lower than 0.3 by the R-point impact. The injury risk correspondingly is 18.60%, and the injury risk of the intestine in the rear impact case is less than half of the R-point impact, which is 7.72%.

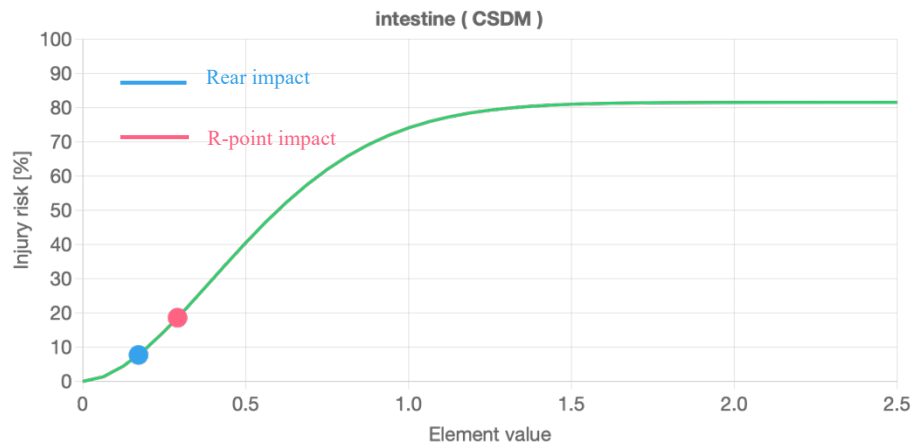


Figure 91 Injury risk value of the intestine on the R-point impact (red) and the rear impact (blue)

Chapter 5: conclusion

In this thesis work, injury risk of the occupant in the vehicle during the side impact accident is studied based on finite element model analysis. Two scenarios are considered and studied, which are the R-point side impact, and the rear wheel axis side impact. The configuration of the simulations is referring to the Euro NCAP. The speed of the movable deformable barrier to impact against the vehicle is 50km/h and heads perpendicular to the vehicle. All the simulations were executed using LS-DYNA.

To analyse the injury risk and biomechanical data of the THUMS in a probabilistic way, a set of software developed by JSOL company was used, after the simulations were successfully completed, including:

- Command-line interface software (CLI)
- Injury risk visualisation tool

For both two simulations, the result showed a satisfaction behaviour, confirmed by the energy analysis and energy ratio. The CLI software was used to extract the strain data of the human body from the LS-DYNA result (d3plot), and a CSV file was generated containing all the biomechanical information that was needed to do the continuous analysis. Afterwards, this file was uploaded to the injury risk visualisation tool for both simulations, where the injury risk of each part of the body was generated, and the injury risk curve was plotted, at the same time, the value of the CSDM was calculated.

Reading the plots in the injury risk visualisation tool, the head region in both cases has a significant severity, for the brain, the rear impact has an injury risk of 99.64% for AIS 5+, using the MPS criteria, about 20% higher than the R-point impact case, which is 80.99%. Reversely, for the skull, the rear impact has a minor injury risk than the R-point impact, but still very severe, which is 88.09% and 100%, respectively. For the facial bone, the MPS value was not significant enough to generate an injury in both cases. The deformation of the neck in the rear impact is twice larger as the R-point impact case approximately, and in both cases, the deformation could lead to an injury problem. The rear impact has up to 90.68% to get injured, the R-point impact has 48.09 %.

Consciously analysing the thorax region, compared to the R-point impact, all the parts for the rear impact case are not seemed to have an injury problem, their injury risks are below 5%. As for the R-point impact, there is one part that shows a significant problem, the right-side of the scapula, which has a 47.81% chance to be injured. The rest parts: the left and right side's clavicle, the left side's scapula, the twenty-four ribs, the sternum, and the thoracic spine, all have slight deformation but do not lead to an injury problem, the risks are around or lower than 5%.

In the region of the abdomen and pelvis, including the left and right side's pelvis, the sacrum, and the lumbar spine. The rear impact case does not show any high risk of getting injured, all the injury risks are well below 1%. However, for the R-point impact, the left and right side's pelvis have a 30.91% probability of getting injured, and the rest of the parts have an analogic situation with the rear impact case.

Arriving in the upper and lower extremity, none of them was going to have an injury problem in the rear impact scenarios, only in the case of the R-point impact, the right-side bone of the lower leg is a risk of 24.53% getting injured in bone fracture.

For internal organs, except the aorta, the lung, and the intestines, all the rest of the organs have different levels of risk to get injured, but overall, the R-point impact case is more severe than the rear impact. The right side of the kidney with a injury risk of 71.8% has the most significant problem in the R-point impact, the stomach has the highest risk of injury with a value of 56.68% in the rear impact case.

Overall, the R-point impact is more dangerous than the rear impact from the result shown. But in any of the two cases, the neck and the head are high-risk areas.

In conclusion, the use of the injury risk visualisation tool allows a fast and direct view of the risk of injury in the human skeleton view, as a tool based on the probabilistic models, the use of the probabilistic models makes up for some shortages of the deterministic models, which are limited in their ability when the prediction of injury occurs in a population with varying physical characteristics. The use of the HBM provided a low budget and potential complete understanding of the human body behaviour during a car accident. Applying these tools gives a preliminary view of different crash scenarios and provides the change of cost reduction during the passive safety system design and beyond. Not only limited to the automotive industry, but

also for the rescue operation of the car accident, with the help of probabilistic injury assessment tool, it is possible to building a specific injury risk database for different crash scenarios on the aspect of different ages, gender, impact position, etc. With this kind of database, the injury risk of victim could be assessed in time, the rescue operations would be more efficient and accurate.

References

- [1] National safety council "injury facts, 2019"
- [2] Donata Gierczycka, Brock Watson and Duane Cronin, "Investigation of occupant arm position and door properties on thorax kinematics in side-impact," 2015.
- [3] Euro NCAP, "<http://www.euroncap.com/>"
- [4] Adam J. Golmana, Kerry A. Danelsona, Logan E. Millera, Joel D. Stitzel, "Injury prediction in a side-impact crash using the human body," 2013.
- [5] Euro NCAP, "AE-MDB specification version 1.0," 2013.
- [6] Center for Collision Safety and Analysis (CCSA), <https://www.ccsa.gmu.edu/models/2012-Toyota-Camry/>
- [7] F. Garreli, "Side impact crash studies with FE simulation and Human Body Model" Master's Degree thesis in Automotive Engineering, Politecnico di Torino, a.a. April/2021
- [8] Toyota Central R&D Labs. Inc., "THUMS AM50 Occupant Model Version 4.1," 2020.
- [9] Michael Kleinberger, Emily Sun, Rolf Eppinger, "Development of Improved Injury Criteria for the Assessment of Advanced Automotive Restraint System," 1998.
- [10] Abbreviated Injury Scale 2005 (2008 Updated) Association for the Advancement of Automotive Medicine, Des Plaines, IL.
- [11] Algorithm workgroup: D. Cichos (bast), D. de Vogel (Ford), M. Otto (TUV, "Crash Analysis Criteria Description," vol. V. 2.3, 2013.
- [12] Kemper, A.R., McNally, C., Kennedy, E.A., Manoogian, S.J., Rath, A.L., Ng, T.P., Stitzel, J.D., Smith, E.P., Duma, S.M., Matsuoka, F., "Material properties of human rib cortical bone from dynamic tension coupon testing", *Stapp Car Crash Journal* Vol49 (2005)
- [13] Prasad, P., Mertz, H.J., Dalmotas, D.J., Augenstein, J.S., Diggs, K., "Evaluation of the field relevance of several injury risk functions", *Stapp Car Crash Journal* Vol54 (2010)
- [14] Forman, J.L., Kent, R.W., Mroz, K., Pipkorn, B., Bostrom, O., "Predicting Rib Fracture Risk with Whole-Body Finite Element Models: Development and Preliminary Evaluation of a Probabilistic Analytical Framework", *Annals of Advances in Automotive Medicine*, Vol56 (2012)
- [15] Bandak, F.A., *On the Mechanics of Impact Neurotrauma: A Review and Critical Synthesis. Journal of Neurotrauma*, 1995. 12(4): p. 635-649
- [16] Takhounts, E.G., Craig, M.J., Moorhouse, K., McFadden, J., "Development of Brain Injury Criteria (BrIC)", *Stapp Car Crash Journal* Vol57 (2013)
- [17] NHTSA (1995) Final economic assessment, FMVSS No. 201, upper interior head protection. www.regulations.gov, NHTSA docket 1996-1762- 0003.

[18] F. Germanetti, "Finite Element Simulation of Impact of Autonomous Vehicle with Human Body Model in Out-of-Position Configuration," Politecnico di Torino, a.a. 2019/2020.

[19] E.G. Takhounts, R.H. Eppinger, J.Q. Campbell, R.E. Tannous, E.D. Power, L.S. Shook, On the development of the SIMon finite element head model, Technical Report, SAE Tech. Pap., 2003.

